NAVWEPS
REPORT 8374
1 February 1963

WATER GAIN BEHAVIOR OF OUTDOOR CLOSED STRUCTURES

by

Gordon S. Mustin

Prepared
for
Bureau of Naval Weapons
RSWI-6
Department of the Navy

Contract NOrd 16687
Task 49-3

Project 400-49(3)

American Scientific Corp.
900 Slaters Lane
Alexandria, Virginia

NAVWEPS
REPORT 8374
1 February 1963

WATER GAIN BEHAVIOR OF OUTDOOR CLOSED STRUCTURES

by

Gordon S. Mustin

Prepared
for
Bureau of Naval Weapons
RSWI-6
Department of the Navy

Contract NOrd 16687
Task 49-3

Project 400-49(3)

American Scientific Corp.
900 Slaters Lane
Alexandria, Virginia

	Page
+2 -1 valves	70
+1 -1 valves	71
+1 -1/2 valves	72
+1/2 -1/2 valves	72
Conclusions	75
Recommendations	76
Literature Referenced	77
Appendix I	I-1

CONTENTS

	Page
Abstract	1
Acknowledgments	2
Introduction	3
Method of Computing Internal Temperatures	5
Values of U_1, U_2, h_{co} and h_r	8
Further Simplification of t_i Estimating Equation	11
Computing R_1 and R_2	13
Computing Incident Direct Radiation	14
Survey of Internal Temperatures	22
Selecting Locations to be Analyzed	22
Computing Water Gain (General)	30
Free Breathing Containers (General Survey)	32
Desiccant Breather Service Life	36
Valved Containers	39
The General Problem	39
The Statistical Problem	42
Selecting the Stations to be Analyzed	54
Results of Computer Runs	57
Unvalved Containers	57
Valved Containers	69

ILLUSTRATIONS

Figure		Page
1	Graphical Solution for ϕ_1 and ϕ_2	12
2	Graphical Solution for $\sqrt{H}$, f_1, f_2, f_3 and f_4	15
3	Water Gain at Various Stations	35
4	Probable Service Life of Breathers	38
5	Temperature at Mobile, Alabama	43
6	n(s) vs Sample Size for Mean Extreme Values	45
7	Basic Computer Routine	49
8	Climate Conversion and Storage	50
9	Daily T_i and T_{low}	51
10	Decision Unit	52
11	Water Gain Calculator and Print Out	53

TABLES

Table		Page
I	Values of Constants a and b	13
II	Distribution of Stations Analyzed	21
III	Detailed Temperature Computations for Oklahoma City	24
IV	Average Internal High Temperatures - 6 Hottest Months	25
V	Average Water Gains per Cubic Foot at Oklahoma City	34
VI	Statistical Data on Stations Analyzed by Computer	55
VII	Semi Annual Water Gains - Free Breathing Container	58
VIII	Annual Water Gains - Free Breathing Container	59
IX	Comparison of Hand and Monte Carlo Results	66
X	Months of Life Per Gram of Desiccant per Cubic Foot	67
XI	Months of Life Per Ounce of Desiccant per Cubic Foot	68
XII	Breathing by +1/2 -1/2 Valves	74

ABSTRACT

A model of the water gain of empty structures stored in the open is derived. Using this model and a modified Monte Carlo procedure, a statistical analysis is made of probable water gains at 12 stations by enclosures which are free breathing and which have check valves set at +2 -1, +1 -1, +1 -1/2 and +1/2 -1/2 psig.

It is concluded that a breather charge of one ounce per cubic foot should give about six months storage life anywhere in the world, assuming adequate container drawdown. Even the +1/2 -1/2 psig valve required no additional desiccant although it might be expected to breathe as much as 38 times per year at Las Vegas, Nevada with 2σ confidence.

The least pressure-vacuum spread which will not adversely affect a reasonable storage life was not discovered.

ACKNOWLEDGMENTS

Thanks are due many persons. In particular, the author is grateful to N. A. Junker, Bureau of Naval Weapons, who patiently arranged essential financial support of a study which turned out to be far more complicated than originally anticipated. Appendix I was prepared in its entirety by M. J. Peterman and R. S. Nelson, Rocketdyne Division of North American Aviation, who graciously agreed to include their results herein for completeness.

Thanks are also due L. L. Miller, now Executive Vice President, Consolidated American Life Insurance Company, for proving that temperatures can be matched to sine curves and for knowledgeable guidance through the maze of modern statistical theory. The hand computations of average water gains at 120 stations were performed by R. L. Billett, now of Space and Information Systems Division, North American Aviation, during summer employment while a student in the School of Packaging, Michigan State University.

Intense interest in an early solution for possible use on current programs produced the enormous contribution of a computer for the Monte Carlo analysis and the programming drudgery by M. Hatae and E. Kleinman, Space and Information Systems Division, North American Aviation.

Without the help of all of the foregoing interested people, this report would still be in the talking stage.

INTRODUCTION

A shipping container in the open is exposed to deteriorating influences such as sunlight, precipitation, water vapor, sand and dust, microörganisms, etc. Design criteria for the various extreme conditions have been published. * (1)

So long as protection of the contents depends upon a sealed barrier, extreme condition values are useful design criteria. When, however, the container is deliberately designed to inhale and exhale air, reliance on extreme conditions produces unrealistic designs.

The gas laws teach that, in a completely sealed container, the pressure will vary with the internal temperature. In designing such a container to be able to go anywhere in the world, it is obviously sufficient to design for the estimated maximum temperature which would be encountered. The estimated minimum low temperature will dictate the maximum vacuum.

For a breathing container, however, maximum pressure is secondary. ** The mass of air exchanged with the surroundings is the governing factor since dry air exhaled will, as temperature drops,

---

* See literature references at end of this report.

** On controlled breathing containers, the relief valve settings will determine the pressures and vacuums developed. On free breathers, back pressure in tubing or desiccant beds will be controlling.

be replaced with air whose water content is characteristic of the environment. Hence it is necessary to evaluate what the internal temperatures might reasonably be expected to be in typical climates. With such internal temperature data it is possible to:

a. Determine desirable valve settings for controlled breathing containers.

b. Evaluate the total water intake load which must be taken up by desiccant in the container and/or in the breather.

This study was undertaken to obtain these design criteria.

METHOD OF COMPUTING INTERNAL TEMPERATURES

In order to standardize results, this report assumes that one vertical surface of the container is exposed normal to the solar azimuth at time of equilibrium.

For thin walled structures, such as containers, Parmelee and Aubele [2] show that instantaneous heat transfer rate (q/a = heat per unit area per unit time) on the sun side can be computed from:

$$\frac{q}{a} = U_1 (t_e - t_i) \qquad (1)$$

where

U_1 = over-all transmission coefficient on the sun side

t_e = the sol-air temperature on the sun side

t_i = the inside air temperature

The sol-air temperature is [3] that temperature which would exist if the entire heat transfer process were occurring by conduction.

Similarly, on the shaded side, which is losing heat, the heat transfer function is

$$\frac{q}{a} = U_2 (t_i - t_{esh}) \qquad (2)$$

where

U_2 = over-all transmission coefficient on the shade side

t_{esh} = the sol-air temperature in the shade

In solving specific problems, it is necessary to consider known areas. For purposes of this study we consider a rectangular cross-section container whose dimensions, reasonably typical of many designs, are $L = 2W = 2H$.

With such a container the area of the top is the same as the area of the side and the combined area of the ends equals the area of the top. For simplicity, exchange between the container and the ground is ignored. This is usually an outward flow during the day. Thus, this omission will result in computing slightly higher internal temperatures, thus producing a conservative effect on water load.

Under these assumptions, the total area losing heat equals the total area gaining heat. Making the further assumptions that equilibrium is reached,* and that one vertical wall of the container is normal to the sun's azimuth, we may write:

$$t_i = \frac{t_e}{1 + \frac{U_2}{U_1}} + \frac{t_{esh}}{1 + \frac{U_1}{U_2}} \qquad (3)$$

---

* This assumption is reasonable for empty containers. It ignores, however, the heat capacity of container contents. For precise computation in specific instances, however, one could make the complete analysis using Fourier integrals. The effect, here, is judged conservative.

Now, Parmelee and Aubele [2] define t_e as

$$t_e = \frac{\alpha I_{dav} - \epsilon R_1}{h_{co1} + h_{R1}} + t_o = \Delta t_e + t_o \qquad (4)$$

where

α = solar absorptivity

ϵ = emissivity at surface temperature T_s

I_{dav} = average direct solar radiation rate on the top and the one exposed side.

R_1 = radiation exchange factor on sun side, made up of the balance between incoming sky radiation and reradiation

h_{co1} = convection coefficient on sun side

h_{R1} = radiation coefficient on sun side

Similarly,

$$t_{esh} = t - \frac{\epsilon R_2}{h_{co2} + h_{R_2}} = t - \Delta t_{esh} \qquad (5)$$

where the subscript 2's refer to shade side coefficients.

Combining (3), (4) and (5), we have

$$t_i = t_o + \frac{\Delta t_e}{1 + \frac{U_2}{U_1}} - \frac{\Delta t_{esh}}{1 + \frac{U_1}{U_2}} \qquad (6)$$

Values of U_1, U_2, h_{co} and h_r

The over-all transmission coefficient is a somewhat variable number made up from convection and radiation coefficients on both sides of the wall and reflecting the thermal capacity of the wall material. For the sun side we have

$$U_1 = \frac{1}{\frac{1}{h_i} + \frac{d}{k} + \frac{1}{h_{co1} + h_{R1}}} \tag{7}$$

and for the shade side

$$U_2 = \frac{1}{\frac{1}{h_i} + \frac{d}{k} + \frac{1}{h_{co2} + h_{R2}}} \tag{8}$$

where

h_i = inside surface coefficient, actually composed of values representing still air convection and radiant exchange with the contents.

d = wall thickness

k = thermal conductivity of wall

h_{co} = outside convection coefficient

h_r = outside radiation coefficient

Inasmuch as the contents are unknown in this case, it is sufficient for engineering purposes to use the generally accepted value h_i = 1.65 which reflects average conditions.

In thin walled aluminum alloy, steel or even plastic containers, it is readily verifiable that the ratio d/k is usually considerably less than .003 and, therefore, can be ignored.*

The value selected for h_{co} will vary with wind velocity, all other things being equal. For purposes of this study still air is assumed to prevail. This condition was selected as being the most severe. The average film coefficient for the sun surfaces was taken [4] as

$$h_{co1} = 0.33 (T_{s1} - T_o)^{0.25} \tag{9}$$

On the shade side, only vertical surfaces are involved so that

$$h_{co2} = 0.27 (T_{s1} - T_o)^{0.25} \tag{10}$$

where t_s represents the surface temperature.

Few data are available on surface temperatures of objects exposed to direct sunlight. There are some indications that they can be very high. For example, $t_s = 198^{\circ}F.$ when $t_o = 120^{\circ}$ have been reported from measurements of aircraft wing surfaces at Tucson.[5] In order to evaluate h_{co}, t_{s1} was assumed to be 65 percent higher than t_o. Shadey side data are lacking but, on thin walled structures, they must be somewhat higher than ambient. We have assumed t_{s2} a constant

---

* For example, low carbon steel has a k of approximately 26.2 BTU/(hr.) (ft.^{2}) (deg. F./ft.). For 1/4" thickness, $d/k_1 = 0.0008$.

five percent higher than t_o.

In computing sol-air temperatures, Parmelee and Aubele[2] define the radiation coefficients by

$$h_{R1} = \frac{\epsilon \sigma (T_{s1}^4 - T_o^4)}{T_{s1} - T_o} = \frac{.15916 (T_{s1}^4 - T_o^4)}{T_{s1} - T_o} \times 10^{-8} \qquad (11)$$

and

$$h_{R2} = \frac{\epsilon \sigma (T_{s2}^4 - T_o^4)}{T_{s2} - T_o} = \frac{.15916 (T_{s2}^4 - T_o^4)}{T_{s2} - T_o} \times 10^{-8} \qquad (12)$$

where

σ = Stefan-Boltzman constant, 0.173×10^{-8} BTU/hr./ft^2/ ^oR

T = temperature, ^oR

For many paints used on specialty containers, and for corrugated fibreboard containers, low temperature emissivity is approximately the same, i.e. $\epsilon = 0.92$.

Values of U_1 and U_2 were then determined graphically and their ratios were also determined graphically. These ratios were found to be essentially constant over a wide range of temperatures with the following numerical values:

$$\frac{U_2}{U_1} = 0.83$$

$$\frac{U_1}{U_2} = 1.21$$

Further Simplification of t_i Estimating Equation

The symbol Δt_e defined in equation (4), contains α, the solar absorptivity. For most surfaces, the absorptivity and emissivity are, to all intents and purposes, the same.* Letting $\alpha = \epsilon = 0.92$, permits us to write

$$t_i = t_o + \phi_1 (\bar{I}_{dov} - R_1) - \phi_2 R_2 \qquad (13)$$

where

$$\phi_1 = \frac{0.5027}{h_{co1} + h_{R1}}$$

$$\phi_2 = \frac{0.4163}{h_{co2} + h_{R2}}$$

Values of ϕ_1 and ϕ_2 are plotted in figure 1 and were used to compute the various average t_i.

* The significant exceptions are white paint, aluminum pigmented paint and unpainted corrosion free surfaces.

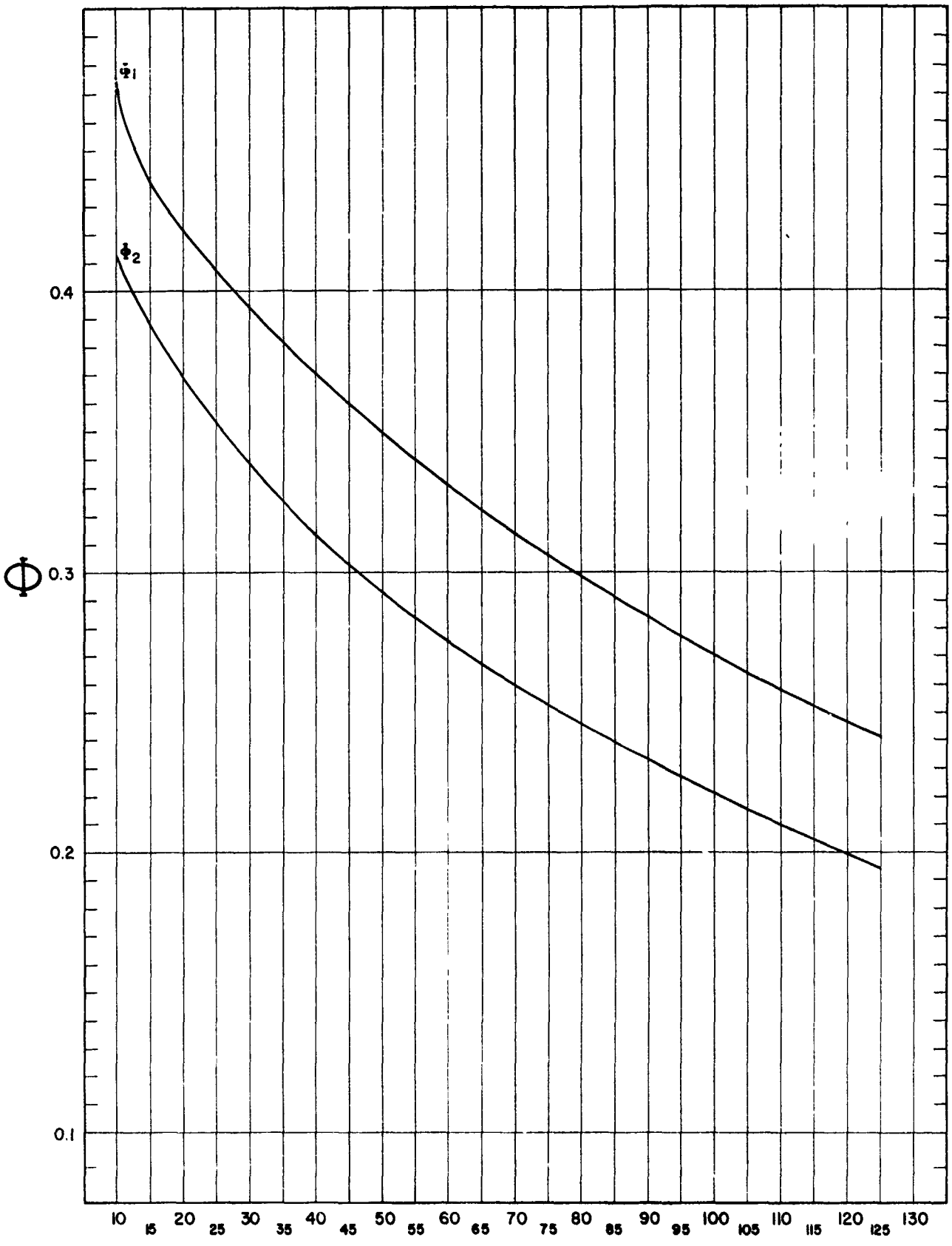

Figure 1 - Graphical Solution for ϕ_1 and ϕ_2

Computing R_1 and R_2

Brunt (6) estimates incoming scatter radiation R_s by

$$R_s = \sigma T_o^4 (a + b\sqrt{p_s H_2}) \tag{14}$$

where

a, b = empirically determined constants tabulated in Table I.

P_s = saturation vapor pressure at T_o.

H_2 = decimal relative humidity at T_o.

TABLE I

VALUES OF CONSTANTS a and b
(After Dines[7])

	a	b
Vertical surfaces	0.30	0.165
Horizontal Surfaces	0..50	0.34
Average for Equal Area Surfaces	0.40	0.253

The net reradiation factor, R_i, is the difference between black body radiation at T_o and R_s, or

$$R_i = \sigma T_o^4 (1 - a - b\sqrt{p_s H_2}) \tag{15}$$

Hence, we have, on the sun side

$$R_1 = T_o^4 (.104 - .043769\sqrt{p_s H_2}) \times 10^{-8} \tag{16}$$

and on the shade side

$$R_2 = T_o^4(.121 - .02845\sqrt{p_s\ H_2}) \times 10^{-8} \qquad (17)$$

Equation (15), and its explicit forms (16) and (17), are tedious to compute by hand for a large number of T_o and H. Note, however, that p_s is also a function of T_o and we may write, in functional form

$$R_1 = f_1(t_o) - f_{i+2}(t_o)\sqrt{H_2} \qquad (18)$$

in which

$$f_1(t_o) = .104\ (T_o)^4 \times 10^{-8}$$

$$f_2(t_o) = .121\ (T_o)^4 \times 10^{-8}$$

$$f_3(t_o) = .0438\ (T_o)^4\sqrt{p_s} \times 10^{-8}$$

$$f_4(t_o) = .0285\ (T_o)^4\sqrt{p_s} \times 10^{-8}$$

Values for $\sqrt{H_2}$, f_1, f_2, f_3 and f_4 are plotted in Figure 2.

H_2 and t_o are taken from the climatic data, p_s from the steam tables, and, with the aid of figure 2, R_1 and R_2 are estimated quickly.

Computing Incident Direct Radiation

With the vertical wall normal to the sun's azimuth

$$\left.\begin{aligned} I_{1d} &= I_{dn} \cos \beta \\ I_{2d} &= I_{dn} \sin \beta \end{aligned}\right\} \qquad (19)$$

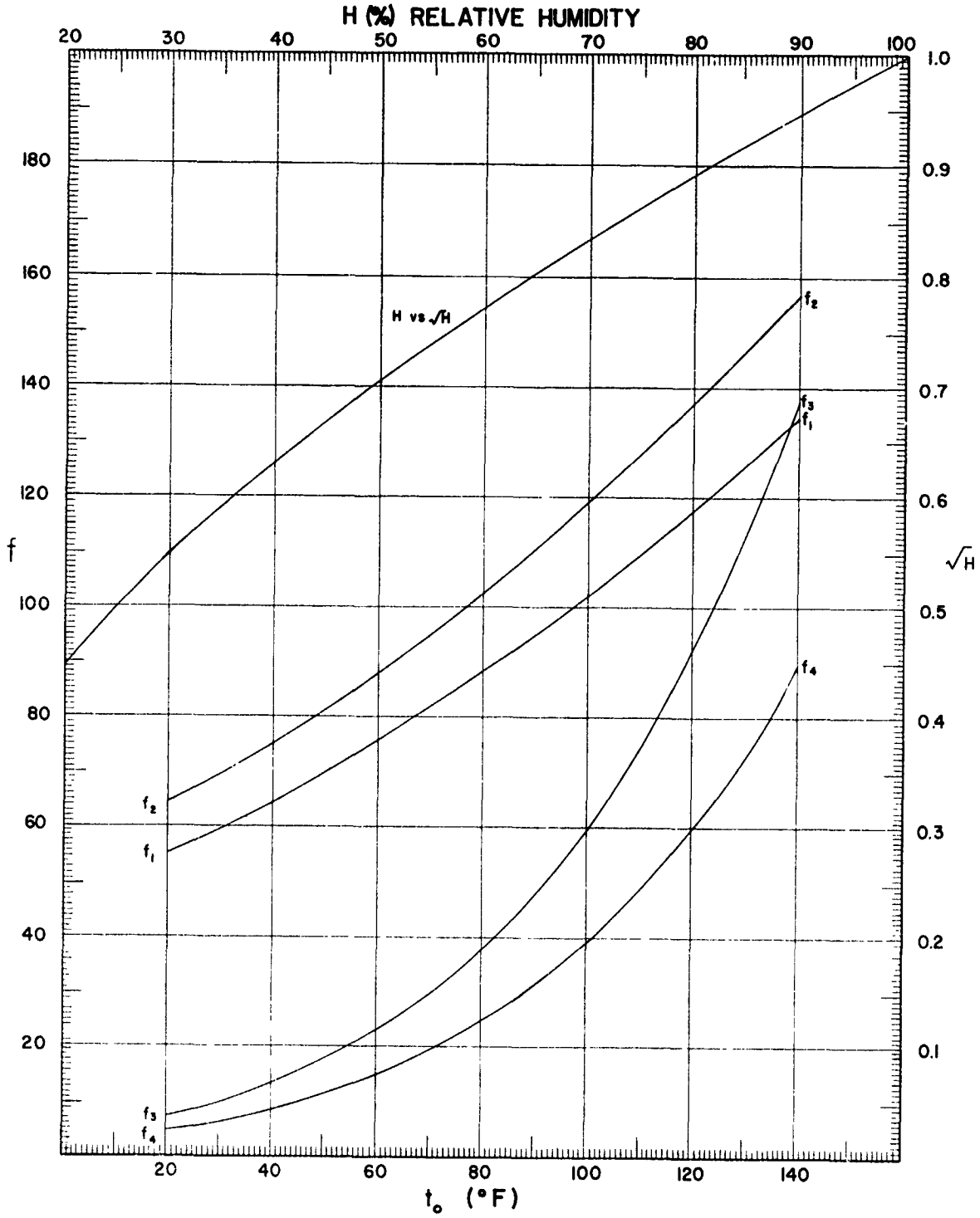

Figure 2 - Graphical Solution for $\sqrt{H}$, f_1, f_2, f_3, and f_4

and, for equal area horizontal and vertical surfaces,

$$I_{dav} = \frac{\sin\beta + \cos\beta}{2} I_{dn} \qquad (20)$$

where

I_{1d} = direct radiation rate on horizontal surface

I_{2d} = direct radiation rate on vertical surface

I_{dn} = direct radiation rate on a surface normal to the sun's rays

β = sun's altitude at the time and place under consideration.

Actual direct solar radiation (I_{dn}) reaching a surface normal to the sun's rays is a highly variable quantity whose value is influenced by the length of the atmosphere traversed by the sun's rays and the components of that atmosphere, particularly water vapor, dust, and carbon dioxide, industrial haze and the amount of cloud cover.

In this study a clear day, free of industrial haze is assumed. Thus, the reducing variables of cloud cover and industrial haze become conservatively eliminated.

Water content of the atmosphere at any given time is not readily predictable. Moisture distribution in the atmosphere is only approximately measured by ground conditions. Moon [8] calculated radiation reaching the surface using 20-mm of precipitable water and estimates that error would be small for other values of water content in our calculations.

Using the foregoing assumptions, direct normal incident radiation can be computed by

$$I_{dn} = T\, I_o = 429\, T \tag{21}$$

where

T = atmospheric transmission coefficient

I_o = normal radiation at the top of the atmosphere. While somewhat variable with the radius vector, the usual value assigned is 429 BTU/ft.^{2}/hr.

Values of T have been computed by Kimball[9] and are reproduced in the Smithsonian Tables [10]. For hand work, the latter reference is preferred. For computer work, however, it was found that the non-linear T function could be matched, in the range of optical air masses to be considered, by the linear function

$$T = 0.86 - 0.09\, m \tag{22}$$

where

m = optical air mass

with error less than 0.01.

For sun altitude greater than 10° ($\beta > 10^\circ$), the optical air mass is computed from [11]

$$m = {}^{p}/_{p_o}\, \csc \beta \tag{23}$$

where

p/p_o = station altitude correction factor taken from the NACA atmosphere tables[12].

Combining (20) through (23), we have

$$I_{dav} = 214.5\ (\sin\beta + \cos\beta)\left(0.86 - \frac{.09}{p/p_a \sin\beta}\right) \qquad (24)$$

Note, here, that negative answers are trivial and should be recorded as zero. So long as $\beta \geq 6^o$, answers will be positive.

Solar altitude, β, can be read directly from tables[13], or in a computer, by solving the well known relationship

$$\sin\beta = \sin L \sin\delta + \cos L \cos\delta \cos h \qquad (25)$$

in which

L = station latitude

δ = sun's declination

h = hour angle at time of equilibrium.

Now, limited studies[14] indicate that T_i maximizes around 3:00 P. M. local sun time. Hence, for this comparative study, it is sufficient to use $\cos h = 0.7071$. In using equation (25), particularly in a computer, it is well to remember that δ can have negative values to the observer when the sun is on the opposite side of the equator.

The value of δ can be estimated from tables of the ephemeris of the sun[15]. As might be expected, it is a sine function with half-

period extending from equinox-to-equinox and with peak amplitude $\pm 23.5^{o}$ (0.4093 radians), occurring at the solstices. Thus, the absolute value of δ on the i th day (d_i) after the spring equinox can be computed from

$$\sin \delta \approx 0.4093 \sin cd_i \qquad (26)$$

where

c = correction factor taking into account different number of days in the various quarters.

The correction constant, c, takes the values 0.978 in the first half-period, $0 - \pi$, and then 0.989 in the interval $\pi - \frac{3}{2}\pi$, and 1.0 from $\frac{3}{2}\pi$ to 2π .

It can be seen that the necessary input data for determining T_i at 3:00 P.M. local solar time have been reduced to:

a. Probable T_o

b. H (expressed decimally) at T_o

c. p_s at T_o

d. station latitude

e. station altitude

f. the date

There are relatively few means of checking whether or not the procedure used is correct. As an exercise, R_s from equation (14)

was computed for Lincoln, Nebraska with input values of average high t_o = 100°F. and H = 0.48 for the month of July taken from the world wide climatic summaries [16]. Sky radiation on a horizontal surface was found to be 143 BTU/sq. ft./hr. The value for I_{1d} for July 17 using the summarized procedure is 192 BTU/sq.ft./hr. Thus the total horizontal radiation is 335 BTU/sq. ft./hr. Mackey [17], for the same location and month, reports measured values of 337 BTU/ft.^{2}/hr. at 2:00 P.M., C.S.T. and 293 BTU/ft.^{2}/hr. at 3:00 P.M., C.S.T. Thus it is apparent that the computed values are as close as can be expected to observed values and that error is on the conservative side.

It should be emphasized that I_{dav} is not necessarily the maximum direct radiation rate but is rather, the radiation intensity at about the time of maximum t_i and t_o. t_o always tends to lag peak insolation (occurring at noon local solar time) because most of the heat of the atmosphere is the result of reradiation in the longer wave lengths from the earth's surface.

TABLE II

DISTRIBUTION OF STATIONS ANALYZED

Climate Class	Description	No. of Stations	Climate Class	Description	No. of Stations
Am	Monsoon	7	Cs	Dry Summer Subtropical	19
Af	Tropical Rain Forest	13	Da	Humid Continental, warm summer	5
Aw	Tropical Savanna	14	H	Undifferentiated highland	2
Bw	Desert	12	Cb	Marine, cool summer	9
Bs	Steppe	12	Db	Humid Continental, cool summer	3
Ca	Humid Subtropical	19	Dc	Sub Arctic	5

SURVEY OF INTERNAL TEMPERATURES

Selecting Locations to be Analyzed

To solve the problem at hand, it is necessary that locations analyzed:

A. Be reasonably representative of the various world climates.

B. Be a reasonably possible storage site (e. g. the top of Mt. Washington is not considered).

C. Have adequate weather data with statistics extending over several years.

Trewartha's (18) modification of the Köppen climate classification system is the classification used in this paper. Frequency distribution of the 120 stations analyzed with respect to 12 climates is shown in table II. Within the climate types, stations were selected with a view to obtaining world wide distribution, insofar as practicable.

Basic source of weather data for the stations selected was the world-wide tables (16). These data are essentially official weather station data and do not necessarily represent the micro-climates close to the ground in probable storage locations. They are, however, the only readily available world wide compilation and, in the absence of more detailed data, must be accepted as representative of true conditions.

As a preliminary step, monthly average internal temperatures were determined for these stations using the middle of the month for δ .

These results were used to compute "average" water gain at each station for free breathing containers in order to characterize the distribution of these water gains by climate types.

Detailed computing results for t_i with intermediate answers, for one station are shown in table III. Table IV contains average t_i for all stations analyzed.

TABLE III

DETAILED TEMPERATURE COMPUTATIONS FOR OKLAHOMA CITY

Latitude 35° Altitude 1254'

Property	May	June	July	August	Sept.	Oct.
Average Ambient Hi (t_o)	78	87	92	92	85	73
Average R.H. at to	.57	.55	.48	.46	.51	.55
Sun's Declination	19° 9'	23° 22'	21° 21'	13° 41'	2° 34'	-8° 58'
Sun's Altitude	47	49	49	44	37	29
Atmospheric Transmissibility	.72	.72	.72	.71	.69	.65
Optical Air Mass	1.30	1.26	1.26	1.37	1.58	1.96
Normal Radiation	309	309	309	305	296	279
Average Direct Radiation (I_{dav})	218	218	218	216	207	190
ϕ_1	.249	.237	.231	.231	.240	.252
ϕ_2	.301	.288	.281	.281	.291	.301
R_1	54	53	52	52	53	56
R_2	80	82	83	83	82	79
Temperature Gain	41	39	38	38	37	34
Temperature Loss	24	24	23	23	24	24
Average Max. Int. Temp t_i	95	102	107	107	98	83

TABLE IV

AVERAGE INTERNAL HIGH TEMPERATURES - 6 HOTTEST MONTHS

Sta No	Name	Yrs. Data	1st Mo	t_i 1	2	3	4	5	6
			Am Climates						
1	Belem, Brazil	16	July	103	104	105	105	105	104
2	Cochin, Indochina	43	Dec	100	100	102	104	105	104
3	Colombo, Ceylon	25	Jan	98	100	102	102	101	100
4	Georgetown, B.Gui.	29	June	101	101	102	103	103	102
5	Manila, P.I.	16	Mar	105	108	108	106	102	103
6	Monrovia, Liberia	3	Dec	100	101	101	103	103	103
7	Rangoon, Burma	60	Dec	96	98	103	109	106	109
			Af Climates						
8	Belize, Br. Hond.	27	May	103	104	104	104	102	101
9	Kieta, Solomon Is.	9	Oct	102	101	102	101	102	102
10	Kuching, Borneo	5	Apr	90	90	91	90	91	89
11	Menado, Celebes Is.	12	May	102	102	101	103	105	105
12	Noumea, New Caled.	22	Nov	97	101	101	100	101	95
13	Penang, Malaya	48	Feb	104	105	105	104	103	103
14	Rio de Janiero, Br.	26	Nov	96	98	100	100	97	93
15	San Juan, P.R.	43	June	100	100	100	101	100	99
16	Stanleyville, Congo	3	Jan	104	104	105	104	103	102
17	Surigao, P.I.	15	Apr	103	104	104	104	104	104
18	Suva, Fiji Is.	31	Dec	101	102	101	100	96	92
19	Tamatave, Madag.	20	Nov	95	96	97	97	96	96
20	Tarawa, Gilbert Is.	5	July	101	103	103	104	103	101
			Aw Climates						
21	Balboa Hts., Panama	33	Dec	100	101	103	105	105	103
22	Bangkok, Siam	16	Feb	105	108	110	108	106	106
23	Bombay, India	60	May	105	104	101	100	99	103
24	Brazzaville, F.Eq.Af.	7	Dec	103	104	105	106	106	104
25	Calcutta, India	60	May	99	104	102	101	99	98

TABLE IV (CONT.)

AVERAGE INTERNAL HIGH TEMPERATURES - 6 HOTTEST MONTHS

Sta No	Name	Yrs. Data	1st Mo	t_i 1	2	3	4	5	6
26	Honolulu, Hawaii	26	June	96	98	98	97	93	89
27	Madras, India	60	May	108	112	111	108	108	107
28	Manaus, Brazil	8	Jul	103	106	107	107	106	105
29	Mandalay, Burma	20	Mar	99	106	105	101	101	101
30	Mombasa, Kenya	45	Nov	96	96	97	98	98	96
31	Nairobi, Kenya	12	Nov	93	93	94	96	96	94
32	Natal, Brazil	6	Dec	100	102	101	101	100	100
33	Port Darwin, Aus.	53	Oct	110	107	105	104	104	106
34	Saigon, Indochina	11	Jan	100	101	104	107	105	104
			Bw Climates						
35	Bahrein, Pers.Gulf	16	May	106	109	112	113	108	100
36	Eilat, Israel	4	May	105	109	110	112	107	98
37	Isfahan, Persia	22	May	98	103	108	106	100	87
38	Karachi, Pakistan	43	May	109	108	107	104	103	102
39	Kazalinsk,USSR	11	May	90	99	102	97	84	63
40	Kuwait City,Arabia	12	May	107	110	111	114	108	98
41	Las Vegas, Nevada	10	Apr	92	101	106	111	111	102
42	Lima, Peru	15	Nov	92	95	98	100	100	96
43	Phoenix, Arizona	9	May	101	108	115	108	107	93
44	Port Said, Egypt	45	May	96	99	102	102	99	93
45	Tashkent, USSR	19	May	93	100	105	101	91	74
46	Tefia, Canary Is.	6	June	95	99	100	95	91	84
			Bs Climates						
47	Ankara, Turkey	26	May	90	94	98	99	90	78
48	Baghdad, Iraq	15	May	107	112	116	115	110	97
49	Berbera, Br. Som.	30	May	110	117	115	114	113	105
50	Dakar, Senegal	16	Jun	104	104	103	105	103	97

TABLE IV (CONT.)

AVERAGE INTERNAL HIGH TEMPERATURES - 6 HOTTEST MONTHS

Sta No	Name	Yrs. Data	1st Mo	t_i 1	2	3	4	5	6
51	Miles City, Mon.	39	Apr	76	86	95	102	100	84
52	Kabul, Afgh.	8	May	95	101	105	103	98	84
53	Jerusalem, Israel	18	May	91	97	101	98	96	90
54	Haifa, Israel	16	May	97	100	102	103	99	93
55	Flagstaff, Ariz.	20	May	86	95	98	96	89	77
56	San Diego, Cal.	59	May	85	88	91	91	88	81
57	Santa Fe, N.M.	54	May	86	94	97	95	89	75
58	Ulan Bator, Mong.	12	May	76	88	95	86	73	54
			Ca Climates						
59	Brisbane, Aus.	52	Oct	94	96	99	98	95	96
60	Buenos Aires, Arg.	23	Nov	91	98	100	98	92	82
61	Chungking, China	13	May	95	101	108	107	97	85
62	Durban, S.Africa	15	Nov	90	92	93	93	90	90
63	Hankow, China	13	May	96	103	108	108	97	87
64	Hongkong, China	50	May	92	94	96	96	93	86
65	Jacksonville, Fla.	59	May	99	103	106	105	100	90
66	Louisville, Ky.	58	May	91	99	103	100	93	78
67	Luang Prabang,Mala	12	Mar	99	102	102	100	98	98
68	Milano, Italy	10	May	89	96	98	96	92	68
69	Mobile, Ala.	30	May	98	103	106	105	99	89
70	Nagasaki, Japan	35	May	91	95	102	104	95	83
71	Norfolk, Va.	60	May	91	97	101	98	93	80
72	Oklahoma City,Okla.	9	May	95	102	107	107	98	83
73	Osaka, Japan	65	May	90	97	102	105	96	83
74	Shanghai, China	38	May	95	99	106	106	96	86
75	Tokyo, Japan	35	May	89	93	100	102	92	78

TABLE IV (CONT.)
AVERAGE INTERNAL HIGH TEMPERATURES - 6 HOTTEST MONTHS

Sta No	Name	Yrs. Data	1st Mo	t_i 1	2	3	4	5	6
76	Venice, Italy	10	May	89	95	97	96	90	73
77	Washington, D.C.	60	May	89	95	97	96	90	78
			Cs Climates						
78	Algiers, Algeria	25	May	88	96	99	99	93	82
79	Athenai, Greece	71	May	92	98	102	100	93	81
80	Beirut, Lebanon	62	May	93	97	101	102	98	88
81	Bizerte, Tunisia	28	May	89	97	102	104	96	86
82	Capetown, S.Africa	19	Nov	86	89	90	91	88	84
83	Erivan, USSR	17	May	92	101	106	105	93	78
84	Famagusta, Cyprus	30	May	96	102	107	108	101	92
85	Iraklion, Crete	21	May	90	95	98	98	93	85
86	Istanbul, Turkey	18	May	85	94	97	96	88	73
87	Lisbon, Portugal	75	May	85	92	94	94	88	76
88	Madrid, Spain	30	May	88	96	102	99	91	75
89	Napoli, Italy	10	May	90	97	100	99	92	78
90	Perth, Australia	43	Nov	91	95	98	97	93	84
91	Nicosia, Cyprus	39	May	96	102	107	107	101	89
92	San Francisco, Cal.	40	May	82	86	85	83	83	78
93	Tangier, Tan.	35	May	87	92	96	95	88	82
94	Valencia, Spain	26	May	89	93	98	97	93	81
95	Valletta, Malta	90	May	88	95	99	100	94	83
96	Valparaiso, Chile	27	Nov	87	88	98	97	92	78

TABLE IV (CONT.)

AVERAGE INTERNAL HIGH TEMPERATURES - 6 HOTTEST MONTHS

Sta No	Name	Yrs. Data	1st Mo	t_i 1	2	3	4	5	6
			Da Climates						
97	Bucaresti, Romania	41	May	90	97	101	100	88	73
98	Cagliari, Sardinia	10	May	88	96	101	99	93	82
99	Pusan, Korea	36	May	86	92	98	100	91	80
100	Roma, Italy	10	May	90	98	102	101	94	80
101	Toulon, France	49	May	87	94	95	95	87	76
			H Climates						
102	Addis Ababa, Eth.	12	Jan	90	92	94	96	95	90
103	Mexico City, Mexico	7	Apr	95	96	96	94	94	93
			Cb Climates						
104	Bordeaux, France	41	May	86	93	94	95	87	74
105	Cherbourg, France	16	May	79	82	85	85	77	62
106	Frankfurt, Germany	50	May	84	89	92	89	79	60
107	Greenwich, England	30	May	80	86	89	86	77	58
108	Koln, Germany	50	Apr	74	83	87	89	86	77
109	Paris, France	24	May	84	89	91	91	86	65
110	Renfrew, Scotland	30	Apr	70	75	82	85	79	71
111	Rotterdam, Neth.	30	May	80	84	87	83	75	60
112	Wellington, N.Z.	65	Nov	82	85	86	85	80	70
			Db Climates						
113	Kiev, USSR	10	May	86	93	94	90	78	58
114	Nemuro, Japan	65	May	73	78	85	87	80	66
115	Vladivostok, USSR	14	May	76	83	89	91	80	64
			Dc Climates						
116	Archangel, USSR	23	Apr	37	66	75	80	79	55
117	Churchill, Manitoba	15	May	63	71	84	76	59	35
118	Fairbanks, Alaska	13	Apr	58	75	86	88	79	59
119	Goose Bay, Newf.	6	May	70	79	87	81	64	48
120	Petropavlovsk, USSR	7	May	67	73	77	78	68	49

COMPUTING WATER GAIN (GENERAL)

Let

T_1 = temperature at which water stops being inhaled on any given day.

T_2 = = temperature at which water begins to be inhaled.

P_1 = pressure at which water is inhaled.

p_a = partial pressure of air.

p_v = partial pressure of water vapor.

W_a = weight of dry air inhaled per cubic foot of original volume on any given day.

W_w = weight of water inhaled per cubic foot of original volume on any given day.

R = gas constant for dry air, 53, 35 ft-lb/lb/^{o}R.

s = specific humidity of air inhaled.

Then, simple manipulation of the basic P-V-T relationship for a constant volume* and constant inhale pressure, gives

$$W_a = \frac{P_1}{R}\left[\frac{1}{T_1} - \frac{1}{T_2}\right] = \frac{P_1}{R}\alpha \qquad (27)$$

and

$$W_w = s\,W_a \qquad (28)$$

---

* This assumes that the oil canning effect is negligible compared to total volume.

Now, by definition [19],

$$s = \frac{p_v}{1.61\, p_a} = \frac{p_v}{1.61(P_1 - p_v)} = \frac{p_s H}{1.61\, P_1 \left(1 - \frac{p_s H}{P_1}\right)} = \frac{\Gamma}{1.61 P_1} \tag{29}$$

Since the daily amount is small, it is desirable to express W_w in grams. Usual units for p_s and P_1 are inches of mercury such that Γ is a dimensionless number. Combining (27) and (28) we have W_w, in grams, for a given day, by

$$W_w = C_1 \alpha \Gamma \tag{30}$$

where $C_1 = 758.32588.$

For n days, total weight of water inhaled is, obviously, given by

$$W_{wt} = C_1 \sum_{1}^{n} \alpha_i \Gamma_i \tag{31}$$

where the subscripts i denote the days on which water was actually inhaled. On free breathing containers this is every day but this does not necessarily hold when check valves prevent free passage of air, a fact which will become important later.

FREE BREATHING CONTAINERS
(GENERAL SURVEY)

Average Water Gains

In free breathing containers, $T_2 = T_1$ and T_1 = the ambient low reached at night. In computing Γ, the temperature and relative humidity are constantly changing. Composition of the inhaled air may, however, be characterized by taking the average of the high and low relative humidities and p_s at the average of T_1 and T_2.

As noted previously, t_i was determined by hand for each mid-month of the six hottest months for 120 stations. This t_i was taken as the average for the month and the indicated computations were made for each of the 120 stations.

Detailed computing results for one station are shown in table V. Total water gains for all stations are shown in figure 3.

It is particularly interesting to note that the monsoon climate (Am) appears most severe even though the daily temperature change is small. Tropical rainforest (Af) and tropical savanna (Aw) are a close second and third. Further, note the high position occupied by deserts (Bw). In fact, although humid subtropical (Ca) -- typically southeastern United States -- is shown in fourth position because of a higher mean, the extreme high values for Bw are comparable to the more severe

tropical intakes.*

---

* While startling at first glance, this is not unusual. While relative humidity is low, absolute humidity is fairly high and the daily temperature swing is also large. On water content, Trewartha (20) states that Yuma, Ariz. has almost as much water in its air in July and twice as much in January as does Madison, Wisc. in the same months.

Table V

AVERAGE WATER GAIN PER CUBIC FOOT AT OKLAHOMA CITY

Property	May	June	July	Aug.	Sept.	Oct.
Average Ambient High, °F	78	87	92	92	85	73
Average Ambient Low, °F	58	67	71	70	63	52
T_{av}, °R	528	537	541	541	534	522
Saturation Vapor Pressure in Hg.	.690	.935	1.084	1.067	0.546	0.570
Average Internal High, °F	95	102	107	107	98	83
High Relative Humidity	.82	.82	.80	.80	.82	.79
Low Relative Humidity	.57	.55	.48	.48	.51	.55
Average Relative Humidity	.70	.69	.64	.63	.67	.67
Weight of Inhaled Water, Grams/ cu. ft.	.76	.89	1.01	1.01	.79	.51
Cumulative Sum	.76	1.65	2.66	3.67	4.46	4.97

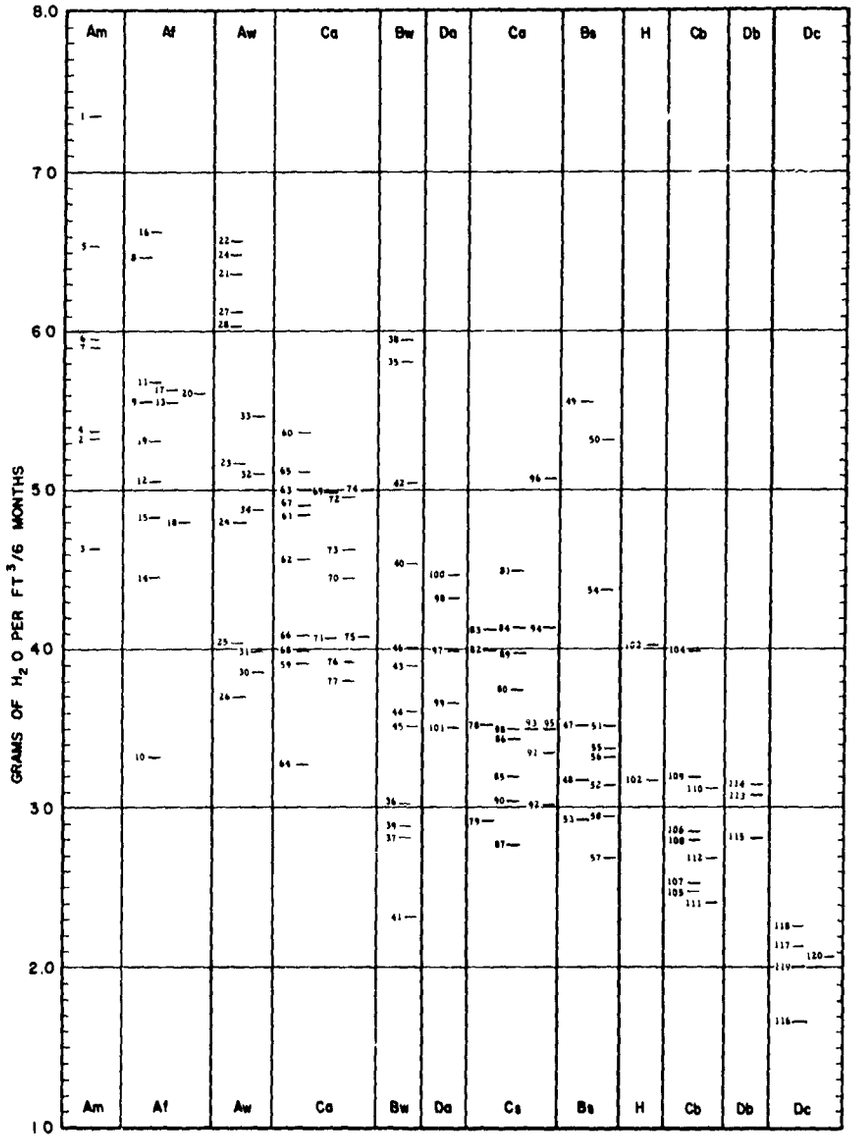

Figure 3 - Water Gain at Various Stations
(Station Key in table IV)

DESICCANT BREATHER SERVICE LIFE

The probable service life of a desiccant breather depends on the water flow in ground storage, the number of flights, the extent of reactivation by dry container air flowing out, the amount of desiccant, and the water sorptive capacity of the desiccant. The latter, in turn, is a function of the point at which the desiccant is considered exhausted.

A general expression for service life in months per gram of desiccant per cubic foot of container volume (M_1) is easily derived as:

$$M_1 = \frac{M_2 \, W_2}{(1 - C)(W_{wt} + n W_3)} \tag{32}$$

where

M_2 = months of exposure. In this study $M_2 = 6$.

W_{wt} = total water gain in time period M_2

W_2 = percentage water storage capacity of desiccant at its end point, expressed decimally.

C = desiccant reactivation factor.

n = number of airplane descents.

W_3 = grams of water inhaled per descent per cubic foot of container.

In preliminary conversations leading up to this work [21], it was agreed that the logical endpoint should be when influent air reaches 40 percent R. H. Thus, using Type I, Grade H, desiccant conforming to

specification [22], $W_2 = 0.215$. Reworking the Peterman and Nelson data given in Appendix I for a free breathing container gives $W_3 = 0.426$ grams H_2O per cubic foot of container volume.

Gelber[23] has made preliminary measurements of reactivation values. Where exhaled air was at 10 percent RH, $C = 0.312$. At 0 percent RH, $C = 0.527$. It is reasonable to assume that a drawdown charge or procedure will be used to reduce container air to 10 percent RH maximum at the time air is being expelled. Hence, $C = 0.312$ is used.

With the foregoing constants, equation[32] reduces to

$$M_1 = \frac{1.875}{W_{w1} + 0.426\,n} \qquad (33)$$

Results are plotted in figure 4.

It is apparent that wide variation in desiccant content is possible depending upon the specific storage conditions assumed.

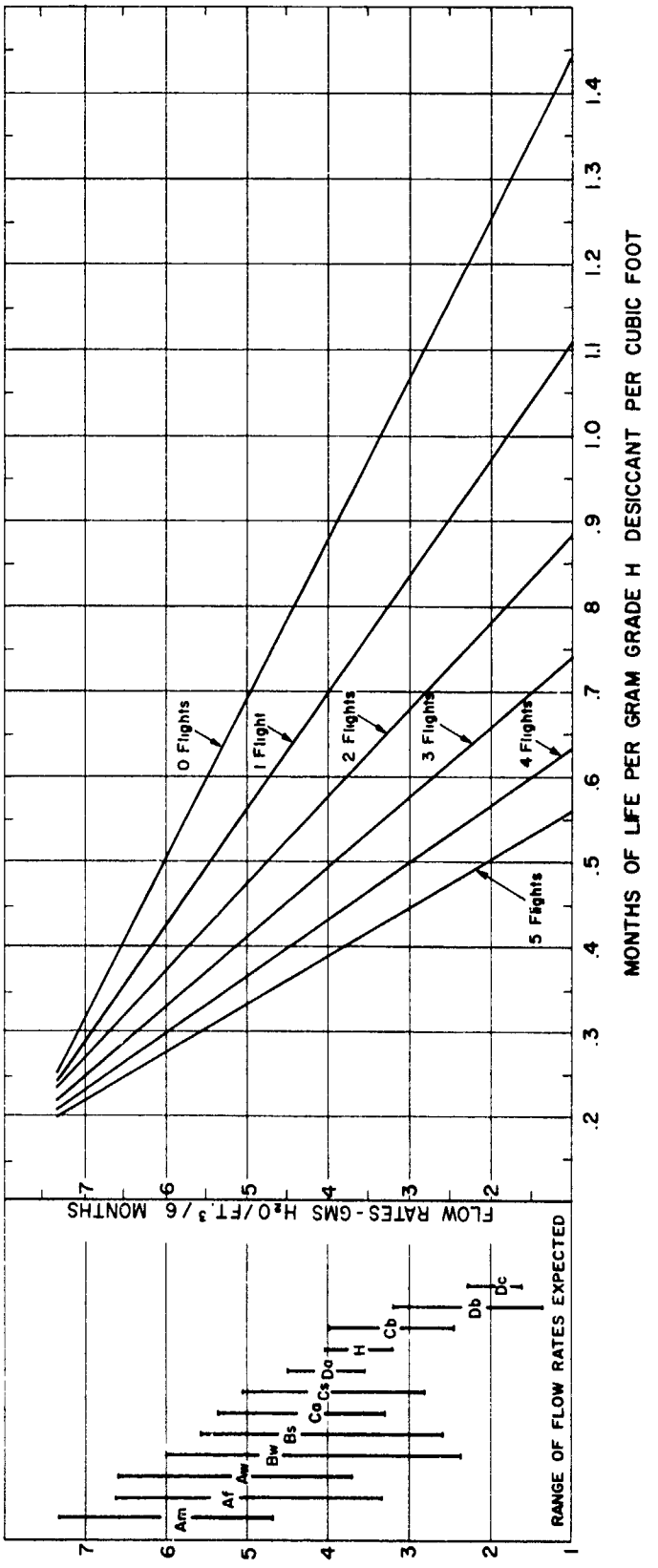

Figure 4 - Probable Service Life of Breathers

VALVED CONTAINERS

The General Problem

Let

T_v = temperature at which the vacuum relief valve opens.

T_p = temperature at which the pressure relief valve opens.

P_p = pressure at which vacuum relief valve opens.

P_v = pressure at which pressure relief valve opens.

T_{low} = ambient low temperature.

T_1 and T_2 are already defined in equation (27).

Then, assuming constant volume, as before, we have

$$T_v = \frac{P_p}{P_v} T_p = T_2 \tag{34}$$

If, and only if, $T_{low} < T_v$ on a given day, the container will gulp water on that day and equations (27) and (31) will come into play with $T_2 = T_{low}$. Note, however, that when $T_{low} < T_v$, the gas law indicates a new T_p for the next day by

$$T = \frac{P_v}{P_p} T_{low} \tag{35}$$

If, however, on this next day, $T_i > T_p$, then we have a new T_v from

$$T_v = \frac{P_p}{P_v} T_i \tag{36}$$

Thus, it is clear that behavior of a valved container, on any given day, is dependent on the past history of the container in a specific climate. It is evident also that reliance on monthly average temperatures to determine water intake over a period of time simply will not give a true picture of the probabilities and will, therefore, fail to provide the information sought herein.*

On valved containers, we are interested in the outcomes (water gains) of a series of possibly highly variable events. In order to arrive at usable design values, we must achieve a statistical distribution of these possible outcomes. The next section will discuss the statistical problem in some detail and demonstrate how a usable answer can be achieved.

Before turning to the statistical problem, it is worthwhile to define the valving arrangements actually considered out of the multitude of those possible. The following configurations were considered since they are representative of feasible commercially available combinations:

---

* It should be noted, further, that even on free breathing containers, we have not yet found the distribution about the mean values computed.

Configuration	Relative Pressure Relief, psig	Relative Vacuum Relief, psig
A	None	None
B	+ 2	- 1
C	+ 1	- 1
D	+ 1	- 1/2
E	+ 1/2	- 1/2

Note that $P_v = P_1$ in equations (27) and (29) and that this pressure is dependent upon the station altitude. Correction for altitude is readily obtained from

$$P_1 = \frac{p}{p_o} P_1' \tag{37}$$

where

P_1' = sea level pressure at which water is inhaled.

The ratios P_v/P_p and P_p/P_v are constant for each valve configuration. Values of P_1' and these ratios are tabulated:

Valve Configuration	P_1' (in. Hg.)	P_v/P_p	P_p/P_v
A	29.92	------	-------
B	27.88	.82024	1.21915
C	27.88	.87234	1.14634
D	28.90	.90426	1.10588
E	28.90	.93369	1.07024

The Statistical Problem

As might be expected from the dependence of I_{dav} on a sine function -- equations (24), (25) and (26) -- mean high and low temperatures can usually be matched to a sine function. Extensive study reveals that the full period, 2π, covers the entire year in the temperate zones. At the equator, on the other hand, the full year encompasses two periods.*

The temperature data in the world-wide tables [16] consist of (among other data), the mean high and low temperatures for each month and the number of years the data have been collected. A typical sine match for one city is shown in figure 5. The matching technique makes the mean of the fitted curve equal to the mean of the empirical data and the area under the fitted curve equal to the area under the data curve. Note that there is a one-month phase angle lag behind the insolation values derived from equations (20), (25) and (26) which is in accord with theoretical expectancy. **

---

* As location approaches the tropics of Capricorn or Cancer, the second period reduces in both amplitude and time duration. In theory this should be taken into account in any computing program. In practice, here, it was not and errors were minimized by taking stations as far north as practicable. Since fluctuations are small in tropical climates anyhow, absolute error is small.

** Once again, it is pertinent to note that heat gain by the atmosphere is primarily the result of reradiation by the earth which is a formidable heat sink.

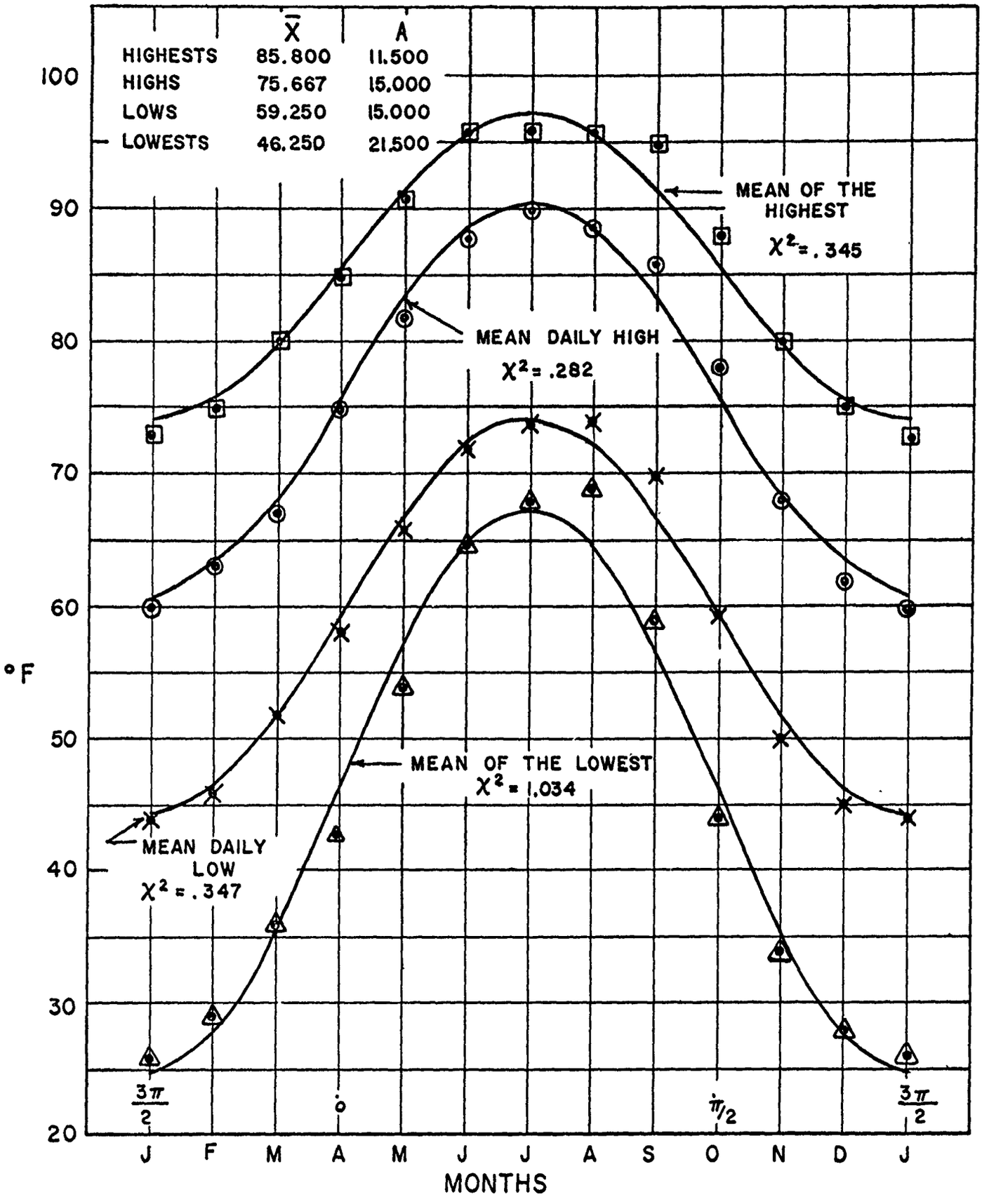

Figure 5 - Temperature at Mobile, Ala.

Once a satisfactory sine curve match is achieved from the tabulated data, then the probable mean high and low temperature for the i th day and the mean of the extreme high and low temperatures for that day are available from

$$x_i = \bar{x} \pm A \sin cd_i \tag{38}$$

where

x_i = expected mean value for the i th day

$\bar{x}$ = annual mean value

A = amplitude of the sine curve, i.e., maximum value of x above or below $\bar{x}$

c = correction factor defined in equation (26)

d_i = the number of days after the day on which $\bar{x}$ occurs, i.e., after April 22.

Thus we have a pair of values representing the mean daily high or low temperature on any given day. We have, further, the number of years of data for each station from the world-wide tables [16] which defines the sample size, n. Now, we have it on good authority [24] that the actual temperature is normally distributed about the mean value after removal of trend values. Thus we are able to use extremal statistical theory to determine the number of standard deviations, n(s), represented by the mean and extreme value pair previously derived. Figure 6, taken from Graph 4.2.2.(4) of Gumbel [25], is the means for

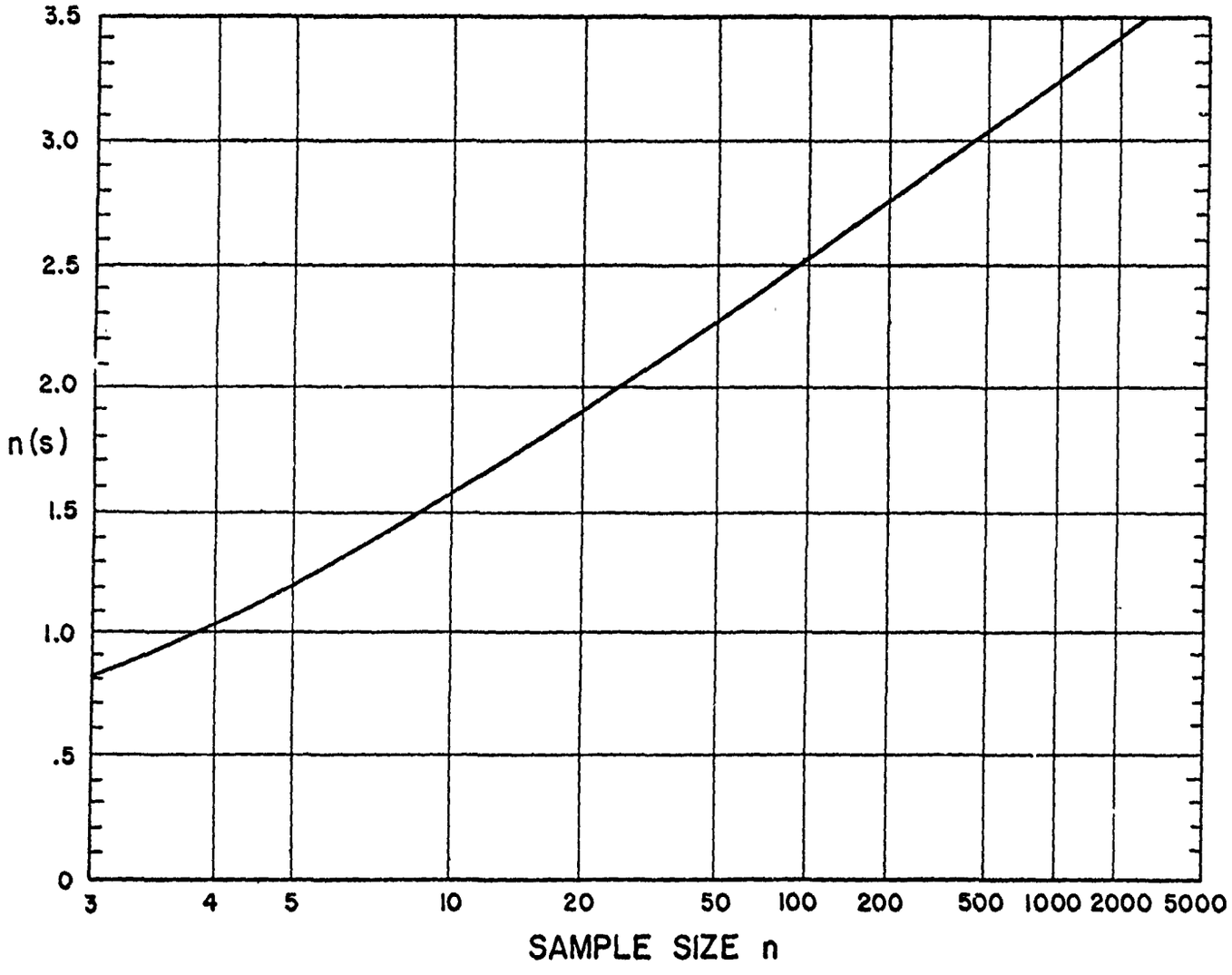

Figure 6 - n(s) vs Sample Size for Mean Extreme Values
(after Gumbel)

accomplishing this statistical operation. Note that n(s) is a constant for each station analyzed.

Now, let

$\bar{x}_1$ = mean high (low) temperature for the year.

$\bar{x}_2$ = mean of the extreme high (low) temperatures for the year.

A_1 = amplitude of mean high (low) temperature curve for the year.

A_2 = amplitude of the average extreme high (low) temperatures for the year.

x_{1i} = mean high (low) temperature on the i th day

x_{2i} = average extreme high (low) temperature on the i th day.

Then, the size of the standard deviation in degrees, s_i, for the high or low temperature on the i th day is given by

$$\left.\begin{aligned} s_i &= \frac{x_{2i} - x_{1i}}{n(s)} \qquad x_2 > x_1 \\ s_i &= \frac{x_{1i} - x_{2i}}{n(s)} \qquad x_1 > x_2 \end{aligned}\right\} \tag{39}$$

Thus, on the i th day, equation (38) gives us the mean high (low) for the day and equations (39) gives the dimensioned standard deviation for that day. These values, coupled with I_{dav} for each day determined from equation (24) constitute a mathematical model of the

day-to-day internal temperature variation inside a container.

It is now possible to construct, for any given day, a reasonable high (low) temperature from the relation

$$t_{o,LOW} = \bar{x}_i + \sigma s_i \qquad (40)$$

where

σ = a signed random normal deviate taken from a table of random normal deviates based on a truly random collection of numbers, e.g., the Rand Table [26].

With t_o thus determined, it is possible to compute t_i and compare the valve settings. With t_{low} it is possible to determine whether or not the valve opens and, if so, how much water is inhaled. Repeating this process 365 times we have a year's water gain for each valve configuration. Repeat for n years at each station and we will have a statistical distribution of water gains covering a sample of size n. From this distribution it is then possible to draw valid statistical inferences concerning the water gain to be expected in specific climates.*

It should be particularly noted that, although high and low temperatures are randomly distributed about their means in a large sample, the high and low temperature on a given date are not completely independent events. Similarly, there is usually about a three day persistence

---

* This, of course, is using the Monte Carlo method in one of its simpler forms. Justifying the validity of using the results of this form of simulating reality is outside the scope of this report.

effect for any given weather cycle. In order to simulate these practical constraints on the chances of extreme variation, use is made of the correlation formula (27)

$$\sigma = \rho\sigma' + \sigma''\sqrt{1-\rho^2} \tag{41}$$

where

σ = correlated new deviate

σ' = previous deviate

σ'' = new random deviate taken from the tables

ρ = degree of correlation

Day and night correlation is set at 90 percent. Correlation between successive days is set at 75 percent for three days, after which a completely new day random deviate is taken.

Equations (1) through (41) thus define a mathematical model of the effects of a climate at any selected location. While each computation is relatively simple, there are a large number of them. Obviously use of a computer is necessary.

A general digital computer arrangement is shown in figure 7.

The climate conversion and storage processes are shown in figure 8 while the operation of generating a daily high internal and low ambient temperature is shown in figure 9. The unit which decides whether or not water is gulped on a given day is diagrammed in figure 10. Water gain

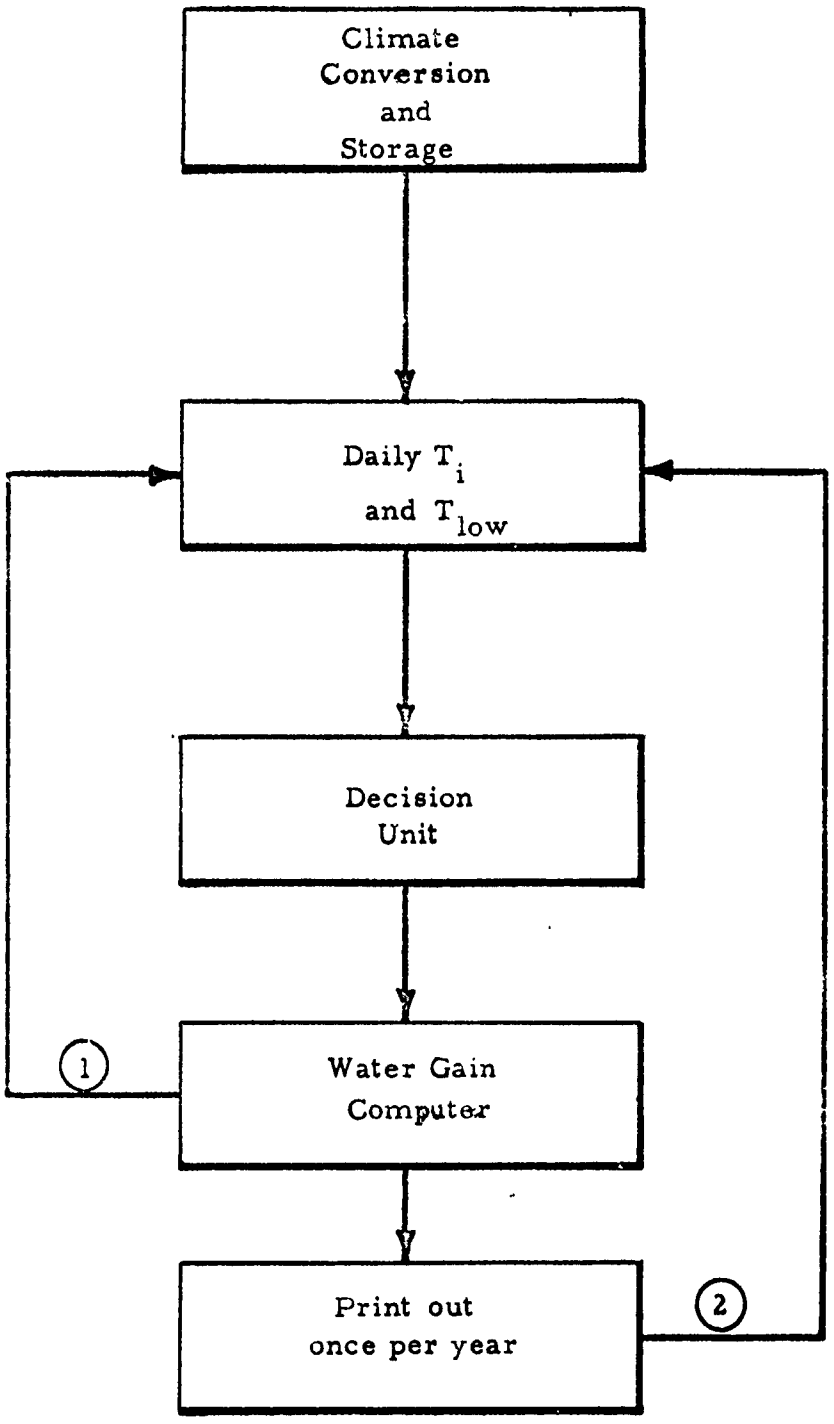

(1) Perform 365 times

(2) Perform n times and stop

Figure 7 - Basic Computer Routine

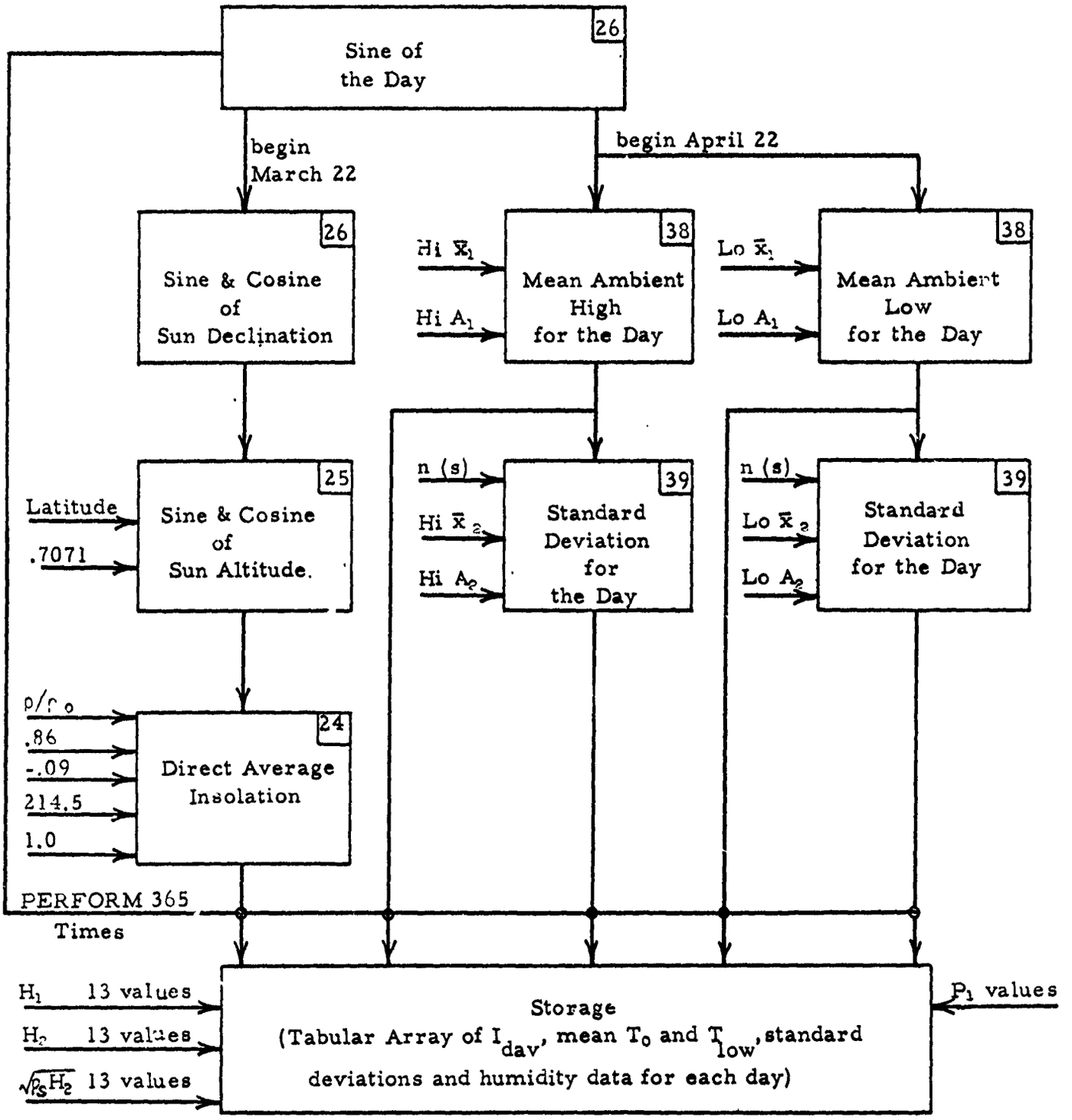

[n] = Number of applicable equation

Figure 8 - Climate Conversion and Storage

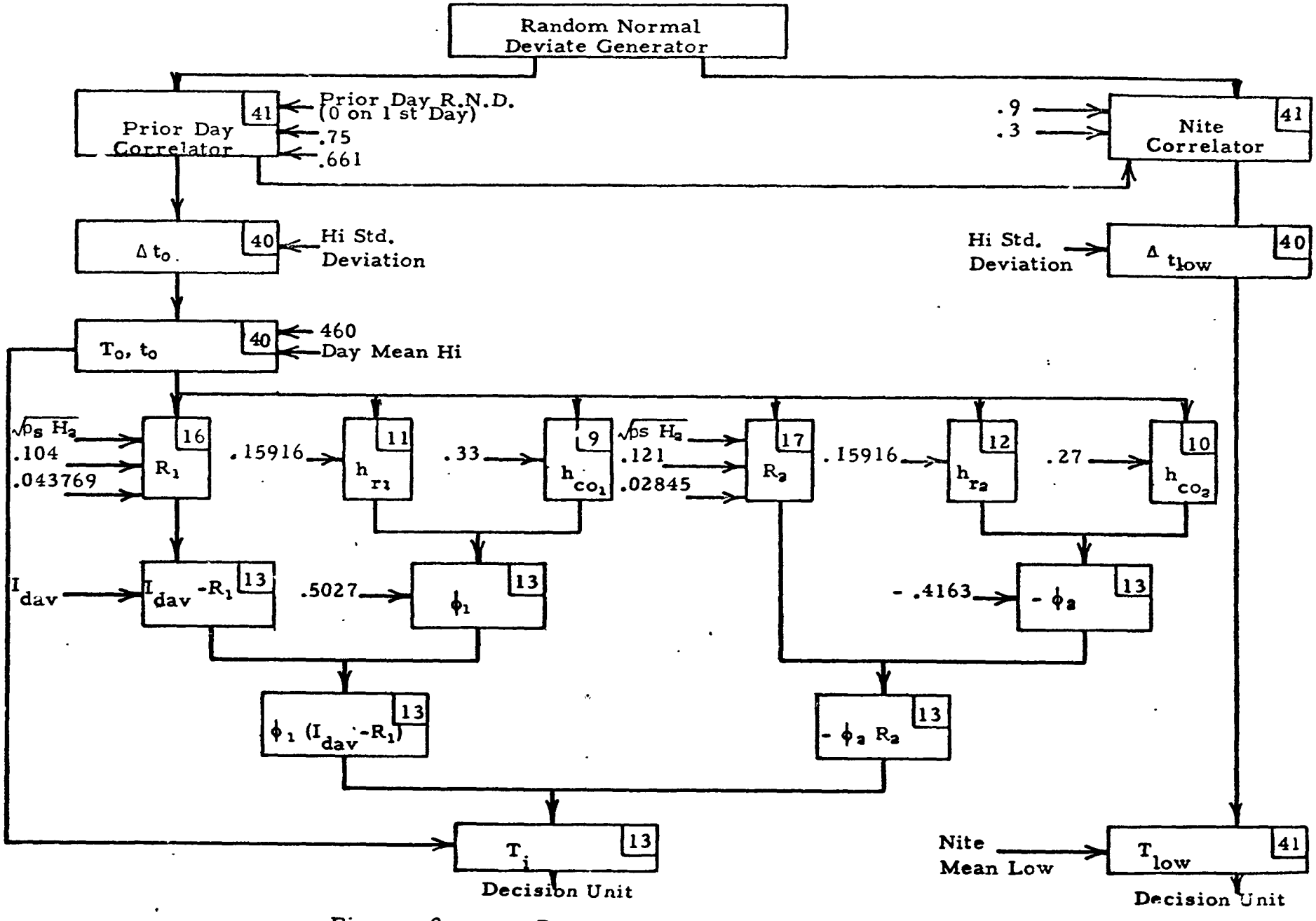

Figure 9 - Daily T_i and T_{low} Generator

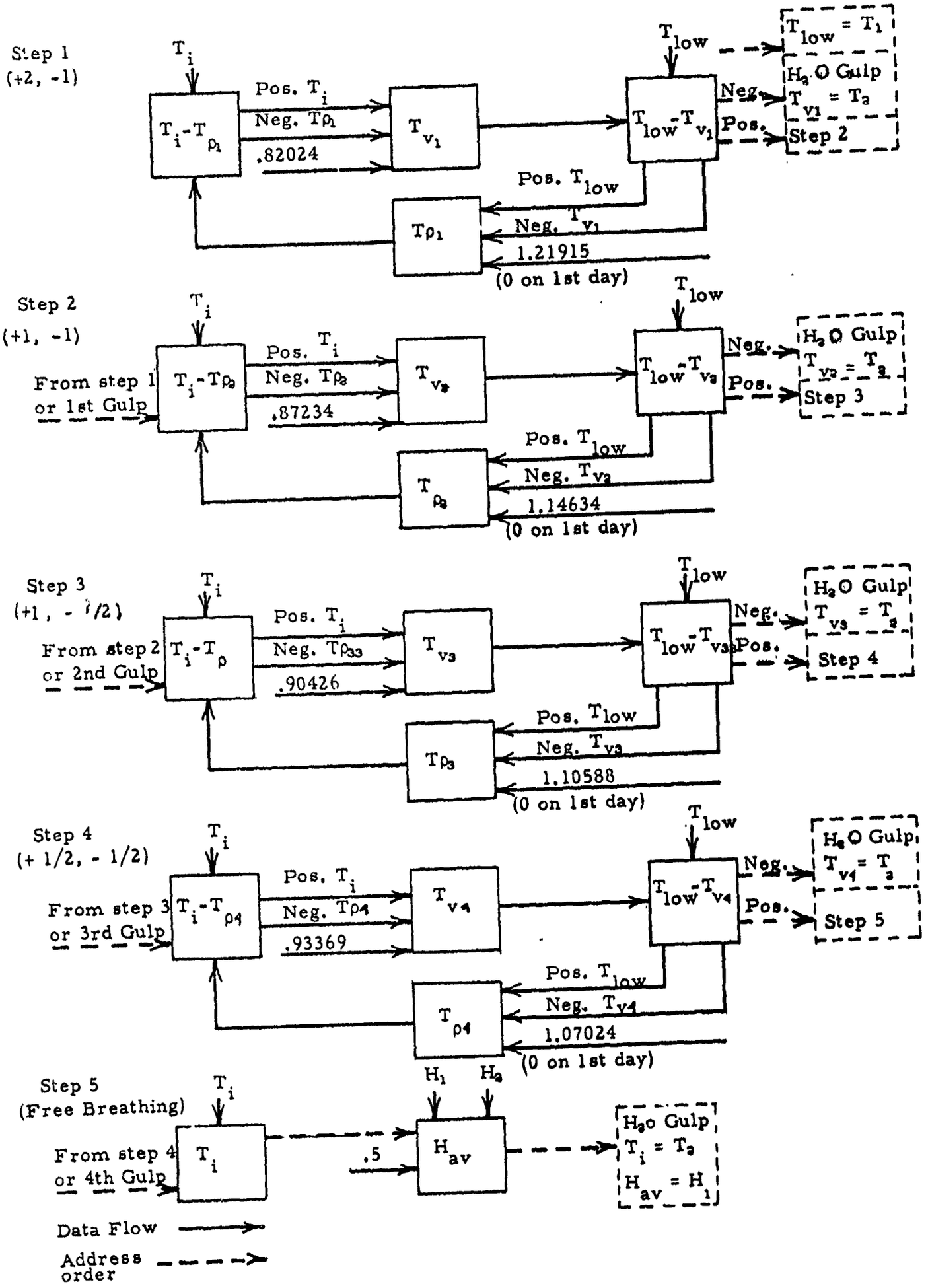

Figure 10 - Decision Unit

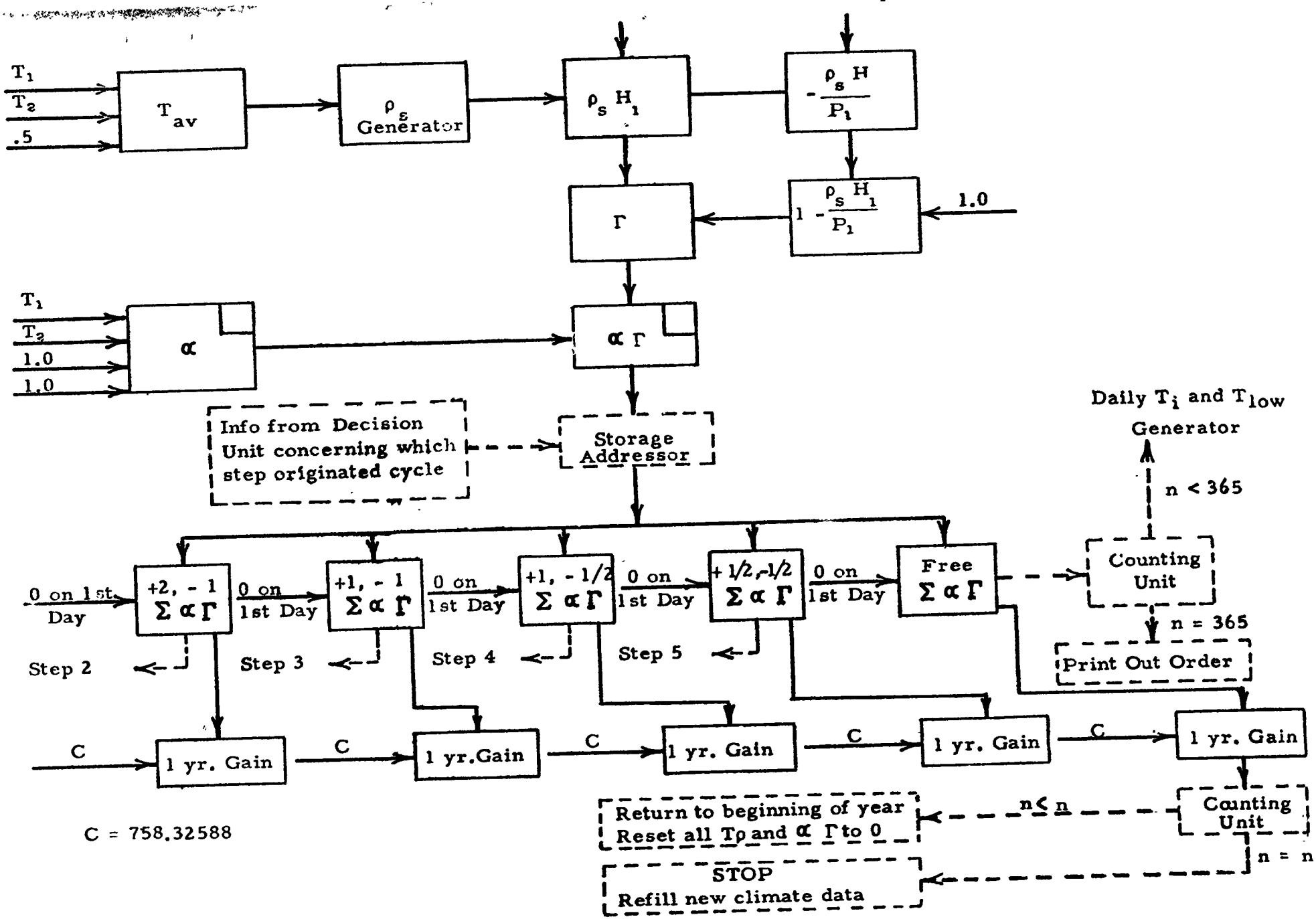

Figure 11 - Water Gain Calculator and Print Out

computation and print out is shown in figure 11.

Actual programming and detailed computations were undertaken by the Space and Information Systems Division of North American Aviation, under the direction of Messrs. Masaji Hatae and Elliott Kleinman.

Since t_i is dependent on t_o, the question will naturally arise concerning why not simply operate statistically on t_i directly. The underlying reason for not doing so is twofold:

a) Transforming t_o to t_i involves a non-linear relation. The basic operators are ϕ_1 and ϕ_2 which vary as shown in figure 1, producing a throttling effect on maximum and minimum t_i. That is to say, the variation in t_i is less than the variation in t_o.

b) The only reasonably statistically valid estimate attainable is the daily mean and standard deviation of t_o.

Selecting the Stations to be Analyzed

While the individual computations diagrammed in figure 7 through 11 are each relatively simple, there are a very large number of them. For obvious reasons, it is necessary to limit the number of stations.

Detailed input data on the stations analyzed are shown in table VI. The following reasoning governed selection:

a. Since we are primarily interested in being able to ship and store anywhere, low water gain climates can be ignored. Based on the

TABLE VI

Statistical Data on Stations Analyzed by Computer

	Manila	Belize	San Juan	Bangkok	Madras	Bahrain	Las Vegas	Berbera	Miles City	Mobile	Wash , D.C.	Famagusta
Station Code	5	8	15	22	27	35	41	49	51	69	77	84
Climate Code	Am	Af	Af	Aw	Aw	Bw	Bw	Bs	Bs	Ca	Ca	Cs
Latitude	14°35'N	17°13'N	18°29'N	18°45'N	13°04'N	26°12'N	36°10'N	10°26'N	46°42'N	30°42'N	38°54'N	35°07'N
Altitude, Ft.	47	17	82	7	51	18	2,400	45	2,392	10	72	75
n(s)	2.30	2.00	2.30	2.13	2.30	1.74	1.88	2.02	2.20	2.45	2.45	2.02
Mean Daily High	88.833	84.917	83.167	90.250	92.000	84.917	82.000	93.917	57.083	75.667	64.750	78.833
Half Range	3.500	3.500	3.000	4.000	8.500	16.500	21.500	11.500	30.000	15.000	22.500	16.500
X^2	1.047	.148	.207	1.419	1.195	1.185	.624	.802	.975	.282	.258	1.663
Mean Daily Low	72.750	71.917	73.083	74.833	74.833	72.000	47.000	77.417	33.833	59.250	46.583	56.000
Half Range	3.000	4.000	3.000	5.000	7.500	14.000	19.500	10.000	26.500	15.000	20.500	14.000
X^2	.085	.180	.169	1.500	.521	.060	1.424	.262	1.292	.347	.676	2.899
Mean of Highests	93.333	88.500	87.750	96.833	96.333	95.583	92.917	98.667	77.667	85.833	81.333	93.333
Half Range	3.000	3.500	3.000	3.500	10.500	14 500	19.500	12.500	26.000	11.500	17.000	18.000
X^2	.707	.113	.219	1.313	1.298	.457	.931	.665	1.029	.345	.486	2.858
Mean of Lowests	68.083	64.333	69.333	67.917	69.833	64.583	37.833	72.167	14.167	46.250	32.083	41.167
Half Range	4.500	6.000	3.000	7.500	6.500	15.500	20.500	9.500	36.000	21.500	25.000	16.500
X^2	.227	.242	.262	1.394	.614	1.461	2.105	.233	1.680	1.034	2.140	3.186
	H_1 H_2	H_1 H_2	H_1 H_2	H_1 H_2	H_1 H_2	H_1 H_2	H_1 H_2	H_1 H_2	H_1 H_2	H_1 H_2	H_1 H_2	H_1 H_2
Rel. Humidity (1)	89 63	92 89	81 75	91 53	87 67	85 71	59 33	87 69	85 69	84 66	73 56	84 72
(2)	88 59	91 87	79 74	92 55	83 66	83 70	56 25	87 70	86 65	83 66	71 53	82 69
(3)	85 55	90 87	76 74	92 56	80 67	80 70	47 21	86 71	84 54	83 62	72 48	75 61
(4)	85 55	91 87	75 75	90 58	74 72	75 66	41 16	89 73	79 45	82 59	68 45	71 57
(5)	88 61	91 87	76 75	91 64	63 67	71 63	31 12	80 66	76 41	82 62	72 48	62 52
(6)	91 68	93 87	76 77	90 67	59 61	69 64	26 10	51 46	77 44	82 62	75 52	59 45
(7)	91 74	93 86	77 78	91 66	65 62	69 67	30 14	45 43	72 37	84 63	79 53	62 45
(8)	92 73	92 87	77 77	92 66	71 66	74 65	32 15	44 46	72 38	86 63	80 53	65 47
(9)	93 73	94 87	78 77	94 70	75 70	75 64	30 13	52 50	77 43	85 62	81 53	64 47
(10)	92 71	94 88	79 76	93 70	83 75	80 56	39 18	78 65	81 49	83 59	81 50	68 54
(11)	91 69	94 91	80 76	92 65	86 75	80 70	49 25	81 66	83 59	83 62	77 51	78 64
(12)	90 67	93 90	81 77	91 56	87 72	85 77	61 35	84 68	84 66	85 68	74 55	80 68

information in figure 3, H, Cb, Db and Dc climates were dropped.

b. The Da climate -- humid continental, warm summer -- appears adequately bracketed by Ca and Cs climates so that stations from the latter two cover the design problem.

c. Stations are taken from the higher valued gains in each climate group because we are seeking a solution to the design problem.

d. Temperature sine curves at a given station should match the empirical data acceptably. The criterion of acceptability was P=0.99 for mean curves and P=.95 for extreme curves using the Chi-squared statistic. With ten degrees of freedom, anticipated values of Chi-squared for these probabilities are 2.558 and 3.940 respectively(28). All curves selected exceed 99 percent significance except the extreme value curves for Famagusta, Cyprus which exceed 95 percent significance. *

---

* Calcutta showed a Chi-squared value of 5.703 on mean extreme highs while Rangoon showed 6.375 and 6.6111 on mean high and mean extreme high. Here, ambient temperature drops at a time when theoretically, it should be rising, apparently because of the onset of the rainy season. Because of poor match, these stations were not analyzed by computer.

RESULTS OF COMPUTER RUNS

Unvalved Containers

Results of computer runs for unvalved containers are shown in tables VII and VII. These tables show, for six months and one year respectively, the mean gain ($\bar{X}$), the sample standard deviation (S) and the various constants needed to compute a distribution curve based on the sample.

Since the a priori distribution function was not known, the Pearson system -- summarized in the literature [29, 30], -- of classification was used. In this system the following properties, based on the first four moments, of the empirical distribution were obtained:

a. The mean, defined by

$$\bar{X} = \frac{1}{n}\Sigma X_i \tag{42}$$

b. The standard deviation

$$S = \sqrt{\frac{\Sigma X_i^2}{n} - \bar{X}^2} \tag{43}$$

c. The skewness

$$a_3 = \frac{\Sigma\left(X_i - \bar{X}\right)^3}{n s^3} \tag{44}$$

d. The peakedness

$$a_4 = \frac{\Sigma\left(X_i - \bar{X}\right)^4}{n s^4} \tag{45}$$

Table VII

Semi Annual Water Gains - Free Breathing Container

	$\bar{X}$	s	a_3	a_4	F_1	l_1	l_2	m_1	m_2	Xm	t (X_m)
Madras	10.64	.06	-.79	2.80	-2.29	.31	-.04	1.84	1.23	10.74	1.67
Manila	10.31	.04	-.81	2.66	-2.67	.39	-.23	.63	-.37	10.37	1.50
Berbera	8.63	.06	-.88	3.18	-1.93	.31	.01	2.27	.07	8.72	1.50
Famagusta	6.44	.10	-.95	3.50	-1.68	.31	.25	2.02	1.63	6.58	1.50
Bahrein	10.72	.12	-.78	3.07	-1.73	1.66	.04	2.97	2.09	10.87	1.25
Bangkok	11.78	.07	-.88	3.04	-2.22	.27	.07	.82	.22	11.89	1.57
Washington	5.57	.08	-.59	2.58	-1.89	.33	.05	1.65	.25	5.80	2.88
Mobile	8.46	.06	-.90	3.11	-2.20	.33	-.03	1.68	-.15	8.57	1.83
Las Vegas	2.40	.06	-.82	3.18	-1.64	.32	.04	3.10	.39	2.48	1.00
Belize	10.83	.07	-.63	2.77	-1.67	.31	.07	2.40	.55	10.97	2.00
Miles City	3.93	.07	-.90	3.59	-1.25	.49	.06	5.82	.72	4.03	1.42
San Juan	7.21	.04	-.47	2.46	-1.76	.13	.04	1.74	.46	7.28	2.14

Table VIII

Annual Water Gains
Free Breathing Container

	$\bar{X}$	s	a_3	a_4	F_1	l_1	l_2	m_1	m_2	Max Value	t(Max)
Madras	21.16	.096	1.92	6.74	-3.62	.47	.52	-.68	-.76	21.62	4.79
Manila	19.16	.044	.50	2.75	-1.25	.07	.20	1.29	3.91	19.28	2.73
Berbera	19.19	.122	2.35	7.94	-6.68	-.23	.85	1.71	.47	19.85	5.4
Famagusta	13.80	1.69	2.75	9.38	-9.95	2.62	4.50	-.56	-.95	23.93	5.99
Bahrein	18.55	.47	2.59	8.57	-8.93	.66	1.31	-.047	-.94	21.29	5.83
Bangkok	21.73	.11	1.76	6.06	-3.18	-.25	1.01	-.46	2.16	22.25	4.64
Washington	9.05	.21	1.88	5.51	-5.60	.10	.75	-.11	-.85	10.08	4.90
Las Vegas	7.17	4.00	2.75	9.14	-10.43	6.64	9.16	-.70	-.97	31.15	6.00
Mobile	14.41	.29	1.75	6.28	-2.59	-.32	2.64	-.44	3.61	14.83	1.45
Belize	20.87	.087	-.53	2.87	-1.10	.48	.18	6.20	2.29	21.05	2.07
Miles City	7.54	.97	2.73	9.37	-9.67	1.43	2.74	-.49	-.95	13.33	5.97
San Juan	13.83	.06	1.44	6.16	+.13	.04	--	.93	--	13.88	.88

In the Pearson system of classification, the first step is to compute the reduced critical function,

$$F_1 = 2a_4 - 3a_3^2 - 6 \tag{46}$$

As shown in the tables the computed value of this function is negative in every case but one and a_3^2 is positive in every case. Thus each distribution curve except that for San Juan is a Pearson Type I, defined, with the origin at the mode, by

$$y = y_0 \left(1 + \frac{x}{\ell_1}\right)^{m_1} \left(1 - \frac{x}{\ell_2}\right)^{m_2} \tag{47}$$

$$y_0 = \frac{n}{\ell} \cdot \frac{m_1^{m_1} \; m_2^{m_2}}{\left(m_1 + m_2\right)^{m_1 + m_2}} \cdot B\left(m_1 + 1, m_2 + 1\right) \tag{48}$$

$$R = \frac{6}{-F_1} \left(a_4 - a_3^2 - 1\right) \tag{49}$$

$$\ell = \frac{S}{2} \sqrt{a_3^2 \left(R+2\right)^2 + 16\left(R+1\right)} \tag{50}$$

$$D = \frac{a_3 \left(R+2\right)}{2 \left(R-2\right)} \tag{51}$$

$$l_1 = \frac{1}{2}\left(l - DR\right) \tag{52}$$

$$l_2 = l - l_1 \tag{53}$$

$$m_1 = \frac{y_1}{1}\left(R - 2\right) \tag{54}$$

$$m_1 + m_2 = R - 2 \tag{55}$$

The Type I distribution function is limited in both directions and is normally skewed. If m_1 and m_2 are approximately equal the curve is nearly symmetrical. If m_1 and m_2 are not small, it tails off at both ends but if both are small it rises abruptly at both ends. If m_1 is negative the curve is J - shaped while if both m_1 and m_2 are negative the curve is U-shaped. l_1 and l_2 are the distances on either side of the mode defining the limits of the curve.

In the semi-yearly curves, no data point exceeds l_2 but this is not true for the yearly values, thus indicating a poor match. Both tables VII and VIII show the maximum value recorded and the number of standard deviations (t) this value represents. It is apparent that maximum t is very high -- in fact these values often could be rejected under Chauvenet's criterion. They have not been rejected, however, because we have no physical basis for doing so, even though we are not able to

draw valid statistical inferences from the data.

In seeking a cause for the difficulty on the one year data, the following appears reasonable:

a. Each year uses exactly the same sequence of random normal deviates at each station.

b. In the programming, only enough random normal deviates were placed on cards to run for 18 years. Between runs, the cards were thoroughly shuffled to produce a new set of deviates. In effect, we have two separate samples drawn from the same universe. For the analysis in tables VII and VIII the computed moments were combined in conventional fashion.

c. In the second half of year six of the second run an unusual combination of random deviates must have occurred since X_{III} invariably is found here. The resulting high water gain changed curves which were normally negatively skewed to positive skew and also increased peakedness significantly. Generation of this unusually high number -- which represents a possible climate -- rendered the data non-homogeneous.

d. The cure for non-homogeneous data from a presumably homogeneous universe is only found by taking a very much larger sample, a proceeding not possible at this time.

e. In effect, we gambled -- from early check runs indicating stability and a very small standard deviation -- that a small sample

would be ample and lost. Fortunately, the sample was sufficiently large that a false sense of security could be avoided.

It is interesting to note that the single wild data point introduces some provocative thoughts. Specifically, although the mean gain for the tropical and monsoon stations is the highest, in accordance with expectancy, the highest single one year gain occurs at Las Vegas, a desert station. Here we have a single year gain of 31.15 grams per cubic foot whereas maximum gain at Bangkok is 22.25 grams per cubic foot. This reinforces the suspicion that desert climates can be as severe, or more so, from a water gain standpoint as any in the world.

We are permitted, however, to assume that the mean water gain is normally distributed about the true mean gain and the standard deviation of this distribution is a function of the sample standard deviations. Thus, for Las Vegas, we have in the one year runs:

$$\bar{X}_1 = 6.489$$

$$\bar{X}_2 = 7.845$$

$$s_1 = .087$$

$$s_2 = 5.654$$

$$y = \bar{X}_1 - \bar{X}_2 = 1.356$$

$$s(y) = \sqrt{\frac{S_1^2}{n} + \frac{S_2^2}{n}} = .942$$

Since y is less than twice s (y), the differences between $\overline{X}_1$ and $\overline{X}_2$ are probably not significant. Hence, we can use the computed mean of the combined sample (7.17) with good confidence that its probable error does not exceed $\pm .318$ grams of water per cubic foot of container volume. The example chosen is the worst case.

It is useful to speculate briefly, on what kind of distribution function could reasonably be expected from a sufficiently large sample (say $n > 200$). The distribution is definitely limited to the left (it cannot be less than zero) and may or may not be limited to the right. Positive skewness is, apparently, probable. Accordingly, a Type I function, possibly degenerating into a Pearson Type III, is indicated. The least likely distribution is the handy normal distribution function.

The single exception to the Type I functions is the yearly gain at San Juan where F_1 is slightly positive. It is convenient here, to assume a Type III distribution function, defined, with the origin at the mode, by

$$y = y_0 \; e^{-\frac{X}{\sigma a}} \left(1 + \frac{X}{l_1}\right)^{\frac{l_1}{\sigma a}} \tag{56}$$

$$y_0 = \frac{n}{l_1} \cdot \frac{\left(1 + \frac{l_1}{\sigma a}\right)^{\frac{l_1}{\sigma a}}}{e^{1+\frac{l_1}{\sigma a}} \, \Gamma\left(1+\frac{l_1}{\sigma a}\right)} \tag{57}$$

$$a = \frac{a_3}{2} \tag{58}$$

$$l_1 = \sigma \frac{4 - a_3^2}{2\, a_3} \tag{59}$$

Curve is limited on the left if a_3 is positive. The curve is usually bell shaped but becomes J shaped when a_3^2 is greater than 4.

Table VIII lists, therefore, only l_1.

It is interesting to compare the hand computed six months values with the machine computed values. The results are shown in table IX.

A detailed investigation of the reasons for the large differences is not necessary. Suffice it to say that the machine computing method gives greater confidence and, for any specific problem, is the preferred method.

Taking the mean values from table VII and substituting into equation (33), we obtain the mean storage lives per gram of desiccant in the breather shown in table X. It is apprent that wide fluctuation in lives is possible depending upon the number of flights encountered and the location. Recasting table X in terms of English units, we have table XI. It is a simple slide rule operation to convert the values of table XI to any other loadings which may be desired.

Table IX

Comparison of Hand and Monte Carlo Results

Station	Hand	Machine	Percentage Diff
Madras	6.12	10.64	+ 75
Manila	6.55	10.31	+ 58
Berbera	5.58	8.63	+ 54
Famagusta	4.18	6.44	+ 55
Bahrein	5.82	10.72	+ 84
Bangkok	6.58	11.78	+ 81
Washington	5.38	5.57	+ 3
Mobile	4.99	8.46	+ 69
Las Vegas	2.32	2.40	+ 3
Belize	6.48	10.83	+ 67
Miles City	5.55	3.93	- 30
San Juan	4.82	7.21	+ 50

Table X

Months of Life Per
Gram of Desiccant Per Cubic Foot

City	n = 0	n = 1	n = 2	n = 3	n = 4	n = 5
Madras	.176	.169	.163	.157	.151	.146
Manila	.181	.174	.167	.161	.156	.150
Berbera	.217	.207	.197	.189	.182	.174
Famagusta	.291	.272	.256	.242	.229	.218
Bahrein	.174	.168	.162	.156	.150	.145
Bangkok	.159	.153	.148	.143	.139	.134
Washington	.336	.312	.291	.273	.257	.243
Mobile	.221	.211	.201	.192	.184	.177
Las Vegas	.781	.663	.576	.509	.456	.413
Belize	.173	.166	.160	.154	.149	.144
Miles City	.477	.430	.392	.360	.332	.309

Table XI

Months of Life Per
Ounce of Desiccant Per Cubic Foot

City	n = 0	n = 1	n = 2	n = 3	n = 4	n = 5
Madras	5.0	4.8	4.6	4.5	4.3	4.1
Manila	5.1	4.9	4.7	4.6	4.4	4.3
Berbera	6.2	5.9	5.6	5.4	5.2	4.9
Farnagusta	8.2	7.7	7.3	6.9	6.5	6.2
Bahrein	4.9	4.8	4.6	4.4	4.3	4.1
Bangkok	4.5	4.3	4.2	4.1	3.9	3.8
Washington	9.5	8.8	8.3	7.7	7.3	6.9
Mobile	6.3	6.0	5.7	5.4	5.2	5.0
Las Vegas	22.1	18.8	16.3	14.4	12.9	11.7
Belize	4.9	4.7	4.5	4.4	4.2	4.1
Miles City	13.5	12.2	11.1	10.2	9.4	8.8

Based upon perusal of table XI, it is recommended that the standard breather loading for world wide distribution be set at one ounce per cubic foot of free air volume.

A safety factor working for better service lives than those indicated is the desiccating ability of the breather tubes themselves. While no complete study of this effect has been made -- and in the author's opinion one should -- Zerr [31] found that five 1/4 x 2-1/2 inch tubes in parallel would reduce relative humidity of 80°F. air from 90 to 76 percent at flow rates as high as 0.4 cubic feet per minute.

At the same time, however, the computations made here assume that the only source of water is outside the container. Water trapped in the container should be purged dynamically, if possible. Otherwise this water, even if initially captured by a static draw down charge, will eventually be shared by the breather desiccant with appropriately shortened life.

Valved Containers

Turning, now, to the check valves, we arrive at some reasonably unexpected results. In early check runs it was found that annual water gains were very low. Accordingly, the program was modified to count the number of times a valve opened in each climate. Where the number of openings was small, the probability of a given number of

openings was computed by the Poisson distribution.

$$P(n) = \frac{e^{-\bar{n}}\,\bar{n}^{n}}{n!} \qquad (60)$$

where

n = number of openings

$\bar{n}$ = average number of openings in the sample

Actually, of course, we are dealing with a binomial problem (open - not open). If the number of trials is large, and the number of openings is fairly high, we can estimate the mean number of openings and the standard deviation in the usual way and determine the 2σ number of openings (representing the 95% probable number of openings) using the normal distribution function. These two methods were used in the detailed analyses for each valve.

+2, -1 valve

This valve practically never opens. It opened twice in Washington, D. C. in 36 years and at no other location. Using formula (60), we find the following probabilities for Washington, D. C.

P one opening is .0523

P two openings is .0016

p three openings is 33×10^{-6}

The mean of the two water gains reported is 0.754×10^{-6} grams per cubic foot, a negligible quantity. Thus the quantity of additional desiccant which may be required is completely controlled by the flight syllabus and is, from Appendix I, .084 units per cubic foot per flight, i.e., 0.504 grams of water per cubic foot per flight. MIL-P-116 required 1.2 units per cubic foot (on an empty container basis) with a total water capacity of about 7.2 grams. Assuming sealing at standard conditions we will have about .0648 grams of water per cubic foot in the air (ignoring sorption on the container walls). Thus, it would require about 14 flights to saturate existing desiccant.

On the basis of the foregoing, it is concluded that a +2, -1 valve needs no additonal desiccant beyond the MIL-P-116 formula.

+1, -1 valve

This valve opens rarely. Total number of openings found at Las Vegas is 17 with mean of .472 per year and S = .784/year. Probability of one opening is .312, of two is .038. Thus normal design value is two openings per year. Mean gain per opening is 0.478×10^{-3} grams per cubic foot, for a total design gain, with 96.2% confidence, of $.856 \times 10^{-3}$ grams per year, again a negligible quantity.

On this basis, additional desiccant for this valve is not required.

+1, -1/2 valve

This valve breathes in Belize, Washington and Las Vegas.

The number of gulps at Belize was two in 36 years. Probabilities are, therefore, the same as previously computed. The mean size of the gulp was $.2389 \times 10^{-2}$ grams per cubic foot, still a negligible amount.

The mean number of gulps per year at Las Vegas is 3.583 with standard deviation 2.476 (maximum number was 11). The design number of gulps is, therefore, nine per year with 98.57% confidence. The mean gain per gulp is $.6624 \times 10^{-3}$ grams per cubic foot. Thus, the design annual gain is $.5962 \times 10^{-2}$ grams per cubic foot. In the light of the reserve capacity required by MIL-P-116, this gain is negligible.

Washington gulped twice, hence probabilities are as before. Mean gulp size was $.3316 \times 10^{-5}$ grams, which may be neglected.

Hence, it may be concluded that this valve configuration is usable without additional desiccant

+1/2, -1/2 valve

This valve breathes in all cities except Manila, San Juan and Bahrein. Breathing probabilities are summarized in table XII.

In all cases, the design gain is negligible.

This last statement deserves some expansion. The design

gain for Las Vegas, where breathing is by far the most prevalent, is .0663 grams of water per cubic foot per year. Since MIL-P-116 requires 1.2 units of desiccant per cubic foot and since each unit will hold six grams of water, it would take something over 108 years for this infiltration to exhaust this desiccant capacity assuming a completely dry container. Even if we assume that 95 percent of the desiccant capacity is consumed on initial draw down, the container life is 5.7 years, which is far beyond most current military storage objectives and is certainly in excess of an assumed six months content reinspection cycle.

Appendix I does not compute gains for this valve configuration. It is, however, somewhat greater than the free breathing unit and somewhat less than the +2, -1 valve. For the latter, we already concluded that effect of five flights on storage life was negligible and so the same conclusion applies here.

Hence, we conclude that the +1/2, -1/2 valve needs no additional desiccant.

Table XII

Breathing by +1/2, -1/2 Valves

City	1	2	3	4	5	6	7
Madras	2	.056	--	1	.9477	$.1691 \times 10^{-2}$	$.1691 \times 10^{-2}$
Manila	0	--	--	0	--	--	0
Berbera	2	.056	--	1	.9477	$.8322 \times 10^{-3}$	$.8322 \times 10^{-3}$
Famagusta	11	.306	--	2	.9657	$.2127 \times 10^{-2}$	$.4254 \times 10^{-2}$
Bahrein	0	--	--	0	--	--	0
Bangkok	1	.028	--	1	.9728	$.2366 \times 10^{-2}$	$.2366 \times 10^{-2}$
Washington	4	.111	--	1	.9005	$.1035 \times 10^{-5}$	$.1035 \times 10^{-5}$
Mobile	2	.056	--	1	.9477	$.2464 \times 10^{-2}$	$.2464 \times 10^{-2}$
Las Vegas	808	22.444	7.805	38	.9767	$.1744 \times 10^{-2}$	.0663
Belize	2	.056	--	1	.9477	$.8896 \times 10^{-2}$	$.8896 \times 10^{-2}$
Miles City	30	.806	.790	2	.9345	1.5540×10^{-2}	3.108×10^{-2}
San Juan	0	--	--	0	--	--	0

Column 1 = Total number of gulps in 36 years.

Column 2 = Mean number of gulps per year.

Column 3 = Standard deviation of column 2. Computed only when necessary

Column 4 = Design number of gulps per year. Probability approximately .95 that this number or fewer gulps will occur.

Column 5 = Computed probability of design number.

Column 6 = Mean water gain per gulp, grams per cubic foot.

Column 7 = Design yearly water gain, grams per cubic foot.

CONCLUSIONS

1. The modified Monte Carlo method used in this study provides a quantitative estimate of water gains by containers stored in the open.

2. For free breathing containers tropical and monsoon climates produce the greatest water gain, with a mean on the order of 21 grams of water per cubic foot per year.

3. Of the U. S. stations investigated, the largest mean gain in a free breathing container was 14.4 grams per cubic foot per year at Mobile, Ala. but the largest single year gain, 31.2 grams per cubic foot, occurred in Las Vegas, Nev. although this was 6 standard deviations away from its mean.

4. For valved containers, greatest gains occur in a desert climate (Las Vegas) with a high steppe (Miles City) a poor second.

5. A breather charge of one ounce per cubic foot should provide about six months life in world wide distribution provided the container and contents are adequately dried.

6. All valve configurations investigated, including the +1/2, -1/2 psig valve, do not breathe enough water to affect storage life of the container, assuming initial desiccant charge conforms to MIL-P-116 and reasonable storage life goals.

7. The least valving configuration which would not adversely affect storage life has not been disclosed by this study.

RECOMMENDATIONS

1. Free breather charge be set at one ounce per cubic foot pending further work on effect of breather tubes and a more complete determination of the distribution function.

2. Work be done on breather tubes to determine their effects. This work should be both experimental and theoretical.

3. The probability distribution function of water gains, for three or four selected stations, be determined with greater precision than has been possible here.

4. Controlled breathing containers be accepted with valving arrangements as low as +1/2, -1/2 psig.

5. A study be made to determine what the least pressure-vacuum spread need be.

6. Container strength requirements be based on the pressures and vacuums developed at maximum flow rate encountered in flight.

7. Maximum rates and pressures for commercially available valves be determined and incorporated in the appropriate container design criteria.

LITERATURE REFERENCED

1. MIL-STD-210B

2. Parmelee, G. V., and W. H. Aubele, Trans. Am. Soc. Heat. and Vent. Engs., 58, 85, 1952.

3. Mackey, C. O., and E. B. Watson, Trans. Am. Soc. Heat. and Vent Engs., 51, 75, 1945.

4. Marks, L. S., ed., Mechanical Engineers Handbook, 5th ed., p. 374, McGraw-Hill Book Co., New York, N. Y.

5. Brooks, C. E. P., Climate in Everyday Life, Philosophical Library, New York, N. Y. 1951.

6. Brunt, D., Suppl. to Qtrly. J. Royal Met. Soc., 66, 1940.

7. Dines, W. H. and L. H. G. Dines, Memoirs Royal Met. Soc., 2, 11, 1927.

8. Moon, P., J. Franklin Inst., 230, 583, 1940.

9. Kimball, H. H., Monthly Weath. Rev., 55, 167, 1927; 56, 394, 1928; 58, 43, 1930.

10. List, R. J., Smithsonian Meteorological Tables, 6th ed., p. 437, Smithsonian Institution Publication No. 4014, First Reprint, Washington, D. C., 1958.

11. Ref. 10., p. 422

12. Brombacher, W. G., NACA Rept. 538, 1935.

13. Hydrographic Office Publication H. O. 214, Supt. Docs., Washington, D. C., 1940.

14. Mueller, M., Modern Packaging, July 1949.

15. Ref. 10, p. 495.

16. Tables of Temperature, Relative Humidity and Precipitation for World, M. O. 617c, H. M. Stationery Office, London 1958.

17. Mackey, C. O., Trans. Am. Soc. Heat. and Vent. Engs., 51, 93, 1945.

18. Trewartha, G. T., An Introduction to Weather and Climate, 3rd. ed., McGraw-Hill Book Co., New York, N. Y., 1954.

19. Ref. 4, p. 354.

20. Ref. 18, p. 273.

21. Minutes of American Ordnance Association Container Design Section, Ad Hoc Committee on Pressure Considerations for Air Transport and Outdoor Storage, 1 June, 1961.

22. Specification MIL-D-3716-2, 28 Dec. 1955.

23. Gelber, P. A., Nav Air Exper. Sta. Rept. No. NAES AML 254200, June, 1946.

24. Thom, H. C. S., Oral Communication.

25. Gumbel, E. J., Statistics of Extremes, Columbia University Press, New York, N. Y., 1958.

26. Rand Corp., The, A Million Random Digits with 100,000 Normal Deviates, Free Press, Glencoe, Ill., 1955.

27. Ref. 26, p. XXIV.

28. Hoel, P. G., Introduction to Mathematical Statistics, John Wiley and Sons, New York, N. Y., 1947, p. 246.

29. Elderton, W. P., Frequency Curves and Correlation, Charles and Edwin Layton, London, 2nd ed., 1927.

30. Davenport, C. B., and M. P. Ekas, Statistical Methods in Biology, Medicine and Psychology, John Wiley and Sons, New York, 4th ed., 1936.

31. Zerr, P. J., Container Laboratories Report No. 9916, 28 Sept. 1956.

APPENDIX I

DESICCANT REQUIREMENTS FOR AIR SHIPPED CONTAINERS

NOTE: The information contained in this Appendix was prepared by M. J. Peterman and R. S. Nelson of Rocketdyne Division of North American Aviation. It was furnished to Reed Research by letter MJP:bc dated 31 August, 1961.

Gracious permission to include these results as a part of the overall report is hereby acknowledged.

A. INTRODUCTION

The AOA container design section Ad Hoc Committee is investigating pressure and desiccant considerations of containers for air transport and outside storage. Rocketdyne was assigned the subject project. Consequently this report covers theoretical calculations which answer the following conditions:

1. How much water per cubic foot of container volume must be absorbed by the desiccant in one ascent and descent presuming no valve, a +2 -1 psi valve, or a +1 -1 valve?

2. What is the relationship between valve cracking pressures and water influx?

B. SUMMARY

Desiccant requirements were calculated for containers having relief valves with various settings under conditions of air shipment. Slow and fast rates of descent were considered.

It was found that a container with a valve having a three psi difference in opening and closing pressure, and under conditions of a slow descent, would require approximately ten percent less desiccant than an unrestricted breathing container. By subjecting this container to a fast descent (2200 ft. per minute used as standard) its desiccant requirements would increase 33%; 18% more than the unrestricted container at fast descent. To verify these findings, calculations were made of a container having a pin hole opening (an extreme case of a container having a small opening and a fast rate of descent). The pin hole container required 49% more desiccant than the unrestricted free breathing container.

C. CONCLUSIONS

When subjected to air shipment, a container having a relief valve with a three psi differential in opening and closing pressures, provides little more moisture protection than a free breathing container. Small changes in the settings of the relief valves considered, produce no significant reduction in moisture transmission into the container.

The closer the optimum flow pressure of the valve is to its cracking pressure, the less moisture intake into the container.

The difference in moisture inhalation between a container with a three psi differential (+2, -1) and one with a two psi differential (+1, -1) is quite small (5%).

D. DISCUSSION

The following assumptions were used as the basis for the calculations.

1. That air behaves as a perfect gas according to Boyle's gas law.

$$\frac{P_1 V_1}{T_1} = \frac{P_2 V_2}{T_2}$$

2. That moisture conditions of figure IV, of MIL-STD-210A, is a valid representation of the actual atmosphere encountered.

   The value of 0.022 pounds of moisture per pound of dry air, representing an approximate dewpoint temperature of 80°F is taken from sea level to the altitude (approximately 8,000 feet) where it becomes the moisture content of saturated air. At higher altitudes the design moisture content is the saturation value corresponding to the temperature and pressure for a given altitude. Above 8,000 feet the humidity decreases quite rapidly.

3. That pressure and temperature conditions of Chart IV of MIL-STD-210A is a valid representation of the actual atmosphere encountered. This chart portrays the standard polar atmosphere.

4. That the air within the container at the start of the calculations has a relative humidity of 40%.

5. That during slow descent conditions, the gage pressure of the container is that of the valve cracking pressure.

6. That during fast descent conditions, the gage pressure of the container is that of the valve optimum flow pressure from 30,000 feet to sea level. At sea level the container pressure rises to that of the cracking pressure.

7. That the time lag in water adsorption caused by desiccant adsorption rates is not a significant factor.

   It is realized that the dessicant will not absorb the water instantaneously and some lag will occur. It is felt that this lag will be relatively short and of little importance.

   Due to the fact that data necessary for the calculations was in the form of graphs, it was impossible to calculate directly the influx of water by means of mathematical equations.

   The amount of water influx was determined by averaging the pressure, temperature, and humidity changes in 3,000 foot increments. Larger increments could not be used because of the exponential shape of the curves.

The method of calculation was as follows:

1. The atmospheric pressure on the outside of the container was decreased to that of 30,000 feet. The inside pressure was calculated from the valve cracking pressure. Assuming that the container temperature drops to that of the outside air,* the pounds of air in the container were then calculated.

   *Air temperature within the plane is greater, although unknown, resulting in an additional safety factor.

2. The atmospheric pressure on the outside of the container was raised in 3,000 foot increments until the valve opened and admitted air. The resultant temperature inside the container was calculated by assuming adiabatic mixing with the incoming air and in proportion to the pressure change inside the container.

3. The pounds of air at the end of each increment were calculated using the resultant temperature and pressure. From this, the pounds of air entering the container were derived.

4. The average altitude for each increment was calculated, and with this, the humidity for the increment obtained from Figure IV of MIL-STD-210A.

5. The pounds of water picked up in each increment was calculated by multiplying the average humidity by the pounds of air inhaled.

6. The total moisture to be adsorbed by the desiccant was obtained by adding the moisture inhaled in each increment.

7. The pounds of moisture was then converted to grams. The units of desiccant required was calculated by dividing the grams of water by six. To maintain a relative humidity of 40% each unit of desiccant (MIL-D-3464) must absorb 6 grams of water.

E. SUMMARY OF RESULTS

A 1,000 cubic foot container requires the following amounts of desiccant for one cycle of ascent and descent from 30,000 feet sea level and maintain a relative humidity of 40% within the container.

	Slow Descent	Fast Descent (2200 feet per minute)
Free Breathing Container (Very large opening)	71 units	71 units
Free Breathing Container (Pin hole opening)	71 units	106 units
Container with Valve (Cracking pressure +1, -1 PSI)	67 units	---
Container with Valve (Cracking pressure +2, -1 PSI) *(Optimum Flow Pressure +4.5, -2.5 PSI)	64 units	84 units
Container with Valve (Cracking pressure +3, -0 PSI)	62 units	

*The optimum flow pressure is the required pressure differential across the valve necessary to allow its rated flow volume.